UNESCO/IHA research project on the

GHG status of freshwater reservoirs

The GHG Reservoir Tool (G-res)

Technical documentation

iha
international hydropower association

United Nations
Educational, Scientific and
Cultural Organization

UNESCO Chair in
Global environmental
change

In cooperation with:

With financial support from:

Recommended citation:
Prairie YT, Alm J, Harby A, Mercier-Blais S, Nahas R. 2017. The GHG Reservoir Tool (G-res) Technical documentation. Updated version 3.2 (2022-12-19). UNESCO/IHA research project on the GHG status of freshwater reservoirs. Joint publication of the UNESCO Chair in Global Environmental Change and the International Hydropower Association. 75 pages.

Table of Contents

1. Introduction

The conversion of a river into a reservoir is amongst the most conspicuous examples of landscape transformation. Although an ancient practice dating back several thousand years, impounding rivers or natural lakes has served multiple purposes, including irrigation, navigation, flood control and more recently in history, power generation. The resulting freshwater reservoirs, like all inland aquatic systems, are active sites of carbon processing, such as exchanges from one carbon species to another, mineralisation to different end-products, gas emissions at the air-water interface, sedimentation, and transport to downstream reaches of the hydrological network. For natural aquatic systems, research of the past decade has shown that their role is disproportionately larger than their surface area would suggest (Cole et al. 2007; Tranvik et al. 2009; Raymond et al. 2013; Borges et al. 2014). Although these systems cover only about a few percent of the terrestrial surface of the Earth, their net contribution to the atmosphere is of the same order of magnitude as the net exchanges that occurs between the oceans and the atmosphere (although in the opposite direction) and greater than the delivery of carbon to the oceans from all rivers combined. Given the global importance of natural systems, it is to be expected that man-made freshwater impoundments may be questioned as to their own GHG (greenhouse gas) footprint, and how it may vary in different regions of the world or under different environmental conditions. This can be an important consideration when planning a new reservoir project or when assessing the ecological footprint of existing ones.

To date, estimates of the GHG footprint for reservoirs where direct measurements have not been undertaken are generally derived by applying averages obtained from limited flux measurements in nearby systems or from systems thought to be 'comparable'. There are several shortcomings with this approach. First, it assumes that the sampled systems are indeed representative of the overall distribution of 'comparable' reservoirs, a potentially tenuous assumption given that measurement campaigns generally target systems where GHG emissions are thought to be potentially problematic. Second, it fails to account for the specific environmental conditions of individual reservoirs. Third, the approach assumes that GHG emissions are constant in time, when there is considerable evidence that they significantly decrease in the early years following impoundment (e.g., Teodoru et al. 2012). Fourth, it also assumes that all measured fluxes can be rightfully attributed to the creation and existence of the reservoir, neglecting the well-known fact that aquatic systems emit GHGs as part of their natural carbon cycling processes. Lastly, it ignores the GHG balance of the landscape prior to flooding. Thus, estimating the GHG footprint of a reservoir or group of reservoirs continues to remain a significant scientific challenge.

From a biogeochemical perspective, the true GHG footprint resulting from the conversion of a river to a reservoir is the difference in net fluxes occurring between the landscape and the atmosphere before and after the landscape transformation, i.e., net GHG footprint. The concept of the net GHG impact of a reservoir is not new, but it is important to understand its full meaning.

The G-res tool uses a unique framework in its attempt to represent only the GHG emissions that are attributable to the introduction of the reservoir in a catchment. The G-res tool's operating principles require the explicit consideration of:

- The GHG footprint of the landscape (upstream catchment, reservoir area, downstream river) prior to impoundment.
- The environmental setting of each reservoir (climatic, geographic, edaphic, and hydrologic).
- The temporal evolution of the GHG emissions over the lifetime of the reservoir.
- Displaced GHG emissions, i.e., emissions that would have occurred somewhere else in the aquatic network regardless of the presence of a reservoir.
- Emissions increasing the net GHG emission impact of the reservoir, but that are the result of release of nutrients and organic matter by human activity occurring upstream of or within the reservoir.

Within these principles, we can thus apply a simple conceptual equation to define the net GHG footprint as:

Net GHG Footprint = [Post-impoundment GHG balance from the catchment after introduction of a reservoir] – [Pre-impoundment GHG balance of the catchment before introduction of a reservoir] – [Emissions from the reservoir due to Unrelated anthropogenic sources (optional allocation)]

This net GHG footprint is thus representing a realistic estimation of the actual emissions exclusively attributable to the reservoir impoundment. It also provides a new global approach showing the emissions for the complete lifetime (100 yr) of reservoirs and not for specific year emissions as obtained with field measurements. Thus, the G-res was not developed as a tool for validation of the field measurements, but to obtain the complete emissions portrait over a reservoir's lifetime.

The following sections describe in detail how each of the components of the simple conceptual equation have been defined and calculated in the G-res tool.

In addition to the change in emissions due to the reservoir itself, G-res considers two additional aspects. Firstly, it includes a limited assessment of construction phase emissions, focusing on the key elements of the infrastructure required to establish a reservoir. This is an important consideration since the works required can be significant and because the emissions associated with the construction phase occur in the present rather than delayed into the future. The assessment included in G-res provides an indicative result for the user to judge the relative importance of this source of GHG emissions. Secondly, G-res includes a method for apportioning the net GHG footprint to the services that the reservoir provides. This method relies on users specifying the services of the reservoirs so that the G-res divides the GHG emissions between these services, attributing their impact or benefit appropriately.

The G-res tool has been implemented as a fully integrated online tool (www.hydropower.org/gres-tool). A complete ***G-res tool User guide*** is available for download at the same web address to accompany and facilitate the step-by-step usage of the online tool.

2. Modelling Approaches

The estimation of the change in GHG emissions associated with different components of the G-res tool requires different approaches appropriate for each domain. They also require different information and analyses. The following sections describe the concepts and general methodology used to derive them.

2.1 Pre-Impoundment GHG Balance Module

2.1.1. Overview

The landscape that will be inundated by a reservoir is, prior to impoundment, a mosaic of different ecological sub-units: forests, wetlands, agricultural areas, settlements, lakes, streams and naturally the main river. Each of these sub-units may have a particular behaviour regarding land use intensity and GHG balances. For example, while a piece of forest generally absorbs CO_2 from the atmosphere through photosynthesis, wetlands not only deposit that carbon as peat, but also typically emit CH_4. Similarly, natural streams, rivers and lakes tend to emit both CO_2 and CH_4 (Figure 1). The overall Pre-Impoundment GHG balance (expressed as $gCO_2e\ m^{-2}\ yr^{-1}$) is evaluated by multiplying the surface area of each land cover sub-unit with a specific emission factor appropriate for both CO_2 and CH_4. These are then summed over a 100-year assessment period and averaged to obtain a mean rate over the entire surface area occupied by the reservoir. For forests on mineral soils, the carbon balance figures from Pan et al. (2011) were applied. For other terrestrial sub-units, the Tier 1 default emission factors from the IPCC (IPCC 2006; 2014) were used, available for nine different land use categories, distinguishing between organic and mineral soils (threshold of 40 kgC/m^2 of Soil carbon content (0-30cm) under impounded area) and four climatic zones, yielding a 9 x 2 x 4 table of emission rates (see Annex III for more details).

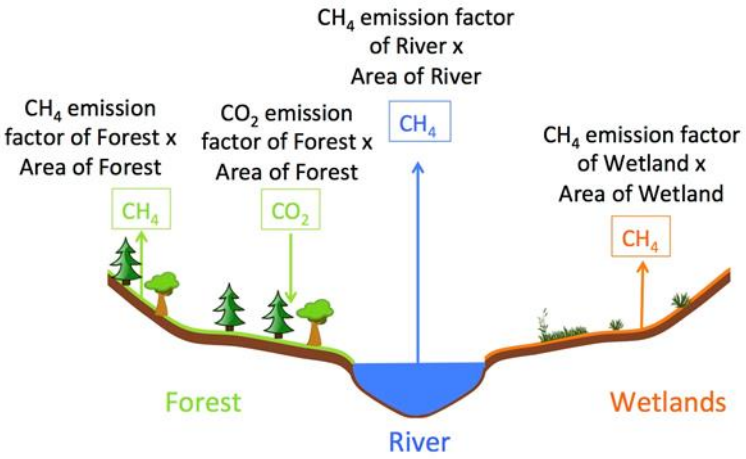

Figure 1: The pre-impoundment landscape as a mosaic of ecological area with different GHG behaviors

For the emission factor of CH_4 from the water bodies present before impoundment, estimates of dissolved CH_4 concentration in water based on size of natural waterbodies (Rasilo et al. 2015) and the corresponding gas exchange coefficients (Vachon and Prairie 2013) (Annex III) were used. The current model does not consider seasonally flooded lands in the pre-impoundment area and their associated (potentially CH_4-rich) GHG regime. Similarly, it does not consider the potentially modulating influence of one reservoir over another in cascading reservoir systems.

2.1.2. Methods to Estimate the Land Cover of the Area to be Inundated

In reservoirs for which the original composition of inundated landscape is known, the general methodology described above can be applied directly. However, for reservoirs for which the original land cover mosaic of the inundated area is not known, a simple proxy has been developed and validated that assumes that the land cover in the immediate vicinity of the current reservoir approximates the pre-impoundment landscape. The method, termed the buffer method, evaluates the land cover of a buffer zone around the reservoir (Figure 2), measuring 25% of the equivalent spherical diameter (analogous to the method of Heathcote et al. 2015). This approach was validated using about 200 reservoirs for which satellite images from both pre- and post-impoundment period were available (Annex IX -).

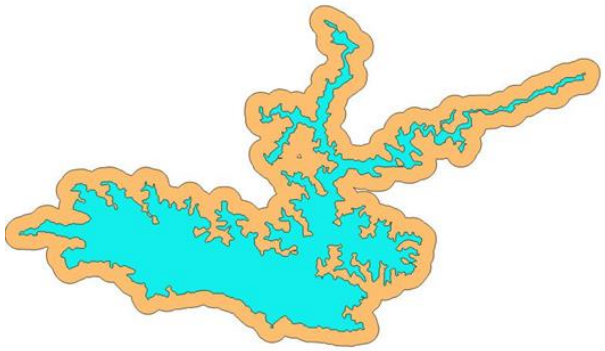

Figure 2: Example of impounded area land cover using the buffer method, the turquoise area representing the reservoir surface area and the orange stripe the 25% of the equivalent spherical diameter. It is calculated as:

$$Buffer\ Width = 0.25 * 2 * \sqrt{\frac{A}{\pi}}.$$

The pre-impoundment module requires information about the area with land use "water" as well as the water body type (lake or river). Information regarding both the size and the type of water bodies existing in the reservoir area before impoundment should be known by the user. Effort should be put into finding local maps of the impounded area before the construction. In case of a planned reservoir, the user will be able to provide this information.

In case of an existing reservoir and if the user cannot find information, satellite images can most likely not be used to obtain the size of the land cover "water", and hence the "buffer method" should not be used to obtain the area of water bodies. This is due to the spatial resolution in satellite images and the fact that water bodies naturally are in the valleys and lower part of all catchments. A buffer around the extremities will then not give a representative picture.

To determine the area with land cover water before impoundment, the following choices can be made:

- If known, the user directly enters the area with land cover water bodies in the inundated area.
- If unknown, the water body in the inundated area has the following characteristics:
  - Assumed to be a river
  - River width is determined by the simple allometric formula (Whipple et al. 2013):
    - $\boldsymbol{W = 5.9 * A^{0.32}}$

- River length is estimated by the user based on the reservoir size (likely the distance from the dam to the upstream river)

The evaluation of the area of land cover with "water bodies" in the inundated area could be improved by analyses on reservoir shore slopes. The pre-impoundment water body type and area is determined by the shore slope in the inundated area. In steep areas rivers are dominant, while in more shallow areas and plains existing lakes were probably present before impoundment.

2.2 Post-Impoundment Emissions Predicting Variables

Unlike the pre-impoundment emissions described in section 2.1 Pre-Impoundment GHG Balance Module, the estimation of the post-impoundment GHG balance of the G-res tool relies on the analysis and the development of semi-empirical models, based on a comprehensive data set collated from the published peer-reviewed literature on measured GHG fluxes. The approach can be viewed in a series of sequential steps. For each GHG flux, estimates are extracted from the literature as follows:

1. Extract the GHG flux data from the literature and record other important information (age of reservoir, method and dates of sample collection, form, and pathway of GHG sampled, other relevant information).
2. Standardize data to annual flux to account for the seasonal variation in temperature and temperature dependency of biological processes.
3. Delineate reservoir boundaries using GIS.
4. Obtain additional data on reservoir from other sources pertaining to climate, geography, and morphometry.
5. Delineate catchment boundaries upstream the dam site using GIS and globally available digital elevation model (SRTM).
6. Obtain additional data on catchment from other sources pertaining to land cover, hydrology, soil properties, and other relevant information.

These steps were completed for all observations, and statistical inference models linking the annual fluxes of CO_2 and CH_4 to both reservoir and catchment properties were developed. Advanced statistical techniques such as the use of elastic net regression, which is particularly well suited to limited data sets containing a long suite of candidate predictor variables, were applied. More details on the steps are provided below and in Annex I.

2.2.1 The Database

Each reservoir used in the development of the model has either CO_2 or CH_4 value (diffusive, bubbling, and degassing flux), and sometimes both. The initial source for the GHG emissions data was the study from Barros et al. (2011). Those data were revised by comparing with the information from the original sources and complemented by data from more recent papers. After a complete review of the actual and past scientific literature on CO_2 and CH_4 emissions from reservoirs, 275 field assessments of diffusive CO_2 emissions, 197 of diffusive CH_4 emissions, 57 of bubbling CH_4 emissions and 51 degassing CH_4 emissions were compiled from 223 reservoirs located in various regions of the world (Figure 3, see Annex VII).

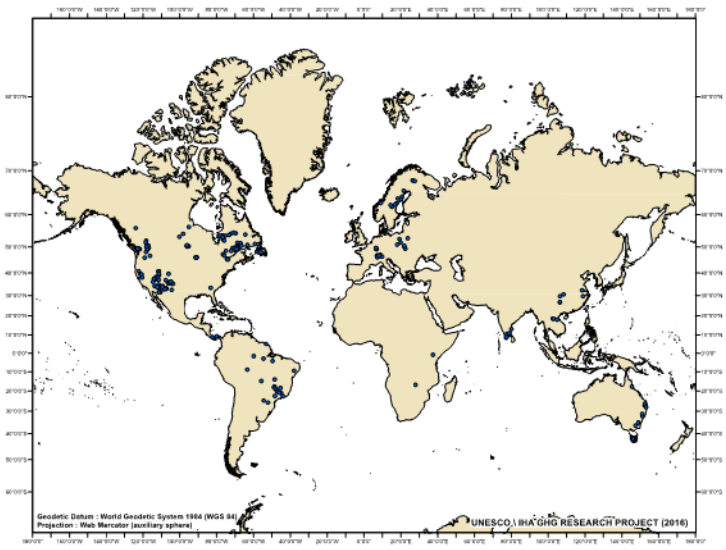

Figure 3: Location of the 223 reservoirs with CO_2 and CH_4 emissions data from the actual and past scientific literature used in the modeling

2.2.2 Standardizing all Literature Estimates to Annual GHG Fluxes

The field assessments of gross GHG emissions found in the literature were not always representative of the annual emissions of the reservoir, as sampling occurred either at a single time point or was averaged seasonally or, in rare cases, annually. In order to standardize all emission values to obtain an annual flux that is commensurate to all reservoirs, a temperature correction coefficient that takes into account the annual variation in temperature together with a factor describing the temperature dependence of GHG production (Liikanen et al. 2013) was used (Annex III). As shown in the literature, both CH_4 and CO_2 production has their own relationship to variation of temperature, production of CH_4 being more highly influenced by variation in temperature than CO_2 (Yvon-Durocher et al. 2014; Inglett et al. 2012).

As shown in Figure 4, the annual variation of GHG flux is then following the seasonal variation in temperature.

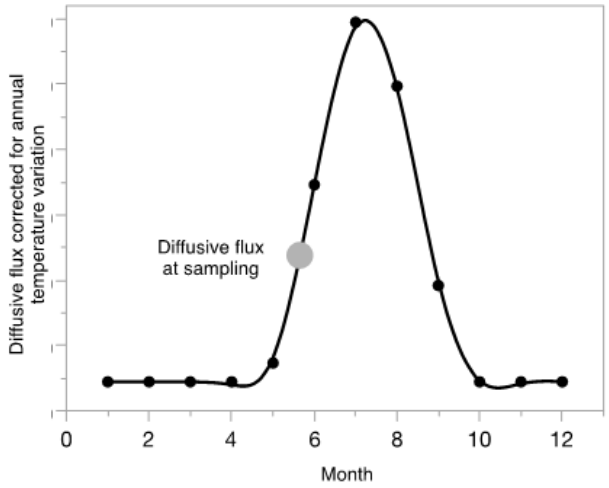

Figure 4: Example of diffusive flux correction from a specific time point flux measurement (Grey dot) to monthly flux (Black dots). The temperature dependence of GHG production will lead to a curve following the natural seasonal variation in temperature over an annual cycle. Averaging the monthly corrected diffusive flux will lead to an annual corrected diffusive flux. The amplitude of the seasonal cycle is most significant in areas experiencing large temperature fluctuations (i.e. temperate and boreal areas)

2.2.3 Complementary Information from the Literature

During this literature review, information such as: Climate; Country; Latitude; Longitude; Year of impoundment; Sampling period; Mean depth; Maximum depth; Reservoir volume; Reservoir perimeter; Reservoir area; Hydroelectric power type; WRT (Water residence time); Water temperature (surface and bottom); Thermocline depth; Annual mean temperature; and Mean annual wind speed, were also compiled from articles to the database if the values were available.

2.2.4 Information Obtained from the GRanD Database

When values for: Mean depth; Maximum depth; Reservoir volume; Year of impoundment; and Coordinates were not available in the literature, Depth; Dam height (proxy used for maximum depth); Capacity; Year; Latitude; and Longitude values from the GRanD database were used. The GRanD database is a GIS layer containing various information on 6,862 worldwide reservoirs of more than 0.1 km^3 of storage capacity (Lehner et al. 2011).

2.2.5 Information Obtained from Global GIS Layer

After determining the surface area and delineating the catchment area of each reservoir, the environmental and geographical information for each reservoir/catchment were extracted, refer to Table 1 (Annex VIII -).

Table 1: List of variables obtained from open access worldwide GIS layers

GIS variables	Units	Source	Supplemental information
Mean monthly and annual air temperature	°C	Global Climate database (Hijmans et al., 2005)	Average for the period 1950-2000
Climate		Rubel and Kottek, 2010 Köppen-Geiger climate classification	4 categories compatible with the emission factor of IPCC (2006): - Tropical - Subtropical - Temperate - Boreal
Annual precipitation	mm yr^{-1}	Global Climate database (Hijmans et al., 2005)	Average for the period 1950-2000
Mean Annual runoff	mm yr^{-1}	Fekete et al., 2000	
Mean monthly and annual wind speed	m s^{-1}	NOAA (GLOBE Task Team et al., 1999)	
Population density	person km^{-1}	CIESIN, 2020	
Soil carbon content of the inundated catchment area	kgC m^{-2}	SoilGrids - global gridded soil information (Hengl et al 2017)	Surface layer of the soil only (0-30 cm)
Land coverage	%	ESA-CCI 2014-2017	9 categories: refer to section 2.2.6 below
Reservoir mean global horizontal radiance	kWh $m^{-2}d^{-1}$	SSE (NASA 2008)	See Annex III to convert to Cumulative global horizontal radiance (kWh m^{-2} $period^{-1}$).

2.2.6 Land Coverage

Global land cover is available from a sophisticated classification algorithm applied to thousands of satellite images and is made available through the European Space Agency – Climate Change Initiative (ESA-CCI 2014-2017). However, this classification produces 36 land cover categories, a number much too high for the degree of precision achievable by the G-res tool. The 36 original land cover categories were amalgamated into several sub-categories into nine broader categories (Annex V):

1. Croplands
2. Forest
3. Grassland/Shrubland
4. Wetlands
5. Settlements
6. Bare Areas
7. Water Bodies
8. Permanent Snow/Ice
9. No Data

For each catchment and reservoir area (when the buffer method was used), the percentages occupied by each of the nine land cover categories above were determined.

2.2.7 Other Calculated Information

In addition to the information about the reservoir and its catchment derived from other sources as described above, we derived estimates of other variables believed to influence

GHG emissions but that were not available directly through other sources. The most important ones were:

Littoral Area (km²) - The littoral area represents the surface area of the reservoir between the shore and the distance to the shore at 3m depth, where the water is shallower and the water temperature warmer than the rest of the reservoir and can be estimated with the maximum and mean depth of the reservoir (Annex III). The % littoral represents the percent of the total reservoir surface area shallower than 3m.

Thermocline Depth (m) - The thermocline is a physical barrier to the movement of matter, nutrient, dissolved gases, and energy. It sets at a depth where the average wind is no longer able to mix the water column. The thermocline depth was calculated using the difference in temperature (density) between bottom and surface water, the surface area of the reservoir, the temperature of air (density) and the wind speed (Gorham and Boyce 1989; Read et al. 2011, Annex III).

WRT (years) - The water residence time (WRT) represents the average amount of time that a molecule of water spends in a reservoir or lake and is essentially a function of the volume of the reservoir relative to the amount of water transiting through it annually (Annex III).

Nutrient status - The GHG dynamics of aquatic systems is highly influenced by the metabolic activity which is in turn a function of the nutrient availability, in particular phosphorus (P) because it is the nutrient most-often limiting biological production in aquatic ecosystem. The concentration of P reached in a reservoir is a direct function of the amount of P it receives through a combination of natural and anthropogenic sources. It is further modulated by the WRT. Reservoirs with short WRT (days to weeks) will tend to have higher concentration relative to their inputs than reservoirs with long WRT (months to year). All the sources need to be accounted for. To this end, P export coefficients (Annex VI) were used from the literature that corresponded to the land cover categories and added human P inputs (2 g day^{-1} person $^{-1}$) based on population density within the catchment:

The sum of all inputs was divided by the discharge (Q = Mean annual runoff / Catchment area) and then subtracted of the retention coefficient.

$$[P] = \frac{P_{\text{Input from catchment}} + P_{\text{Human input}}}{Q} . (1 - R)$$

where P is the estimated steady-state phosphorus concentration in the reservoir, PInput from catchment is the input from each type of land cover (kgP yr^{-1}), PHuman input is the input from human (kgP yr^{-1}), Q is the discharge (m^3 yr^{-1}) and R is the retention coefficient. The tool uses the model of Larsen and Mercier (1976) for Phosphorus Retention:

$$R = \frac{1}{1+\frac{1}{\sqrt{WRT}}}$$

Four categories of water treatment present (if any), representing the percent of phosphorus human input that reaches the reservoir were also included:

- None = No removal, 100%
- Primary = Mechanical removal, 90%
- Secondary = Biological treatment, 30%

- Tertiary = Where additional treatment above primary and secondary is applied, 10%

If no community wastewater treatment is available, the default assumption is that developed countries have a secondary wastewater treatment and that least developed countries (UNDESA, 2018) have no wastewater treatment.

This modelling of reservoir nutrient is a well-known mass-balance approach originally developed for lakes in the 70's and 80's. The approach made it possible to categorize the reservoirs into four broad trophic state categories (Wetzel 2001):

- Oligotrophic = Less than 10 µg L^{-1}
- Mesotrophic = Between 10 and 30 µg L^{-1}
- Eutrophic = Between 30 and 100 µg L^{-1}
- Hyper-eutrophic = More than 100 µg L^{-1}

2.3 Descriptions of the Semi-empirical Models Predicting Post-Impoundment GHG Balance

Using the annualized fluxes of CO_2 and CH_4 extracted from the literature, a series of multivariate statistical models were developed using the reservoir and catchment predictor variables. The elastic net regression procedure allows the optimal selection of useful variables amongst a much longer and complete list of candidate variables. Various transformations were used to satisfy the assumptions of the regression approach, and these resulted in equations (CO_2 and CH_4) to predict the most likely annual emission value for a given set of reservoir/catchment characteristics. All equations took the general form of:

$\log_{10}$ Annual flux = f(predictor variables)

Although the resulting equations are useful to predict the emissions for any given year after impoundment, they do not directly provide estimates of the total emissions over the lifetime of the reservoir (here assumed to be 100 years; IAEA 1995; 1996; Gagnon et al. 2002). As this is often the most relevant metric of the total GHG footprint of the reservoir, we also developed equations to estimate the 100 years integrated emission values. These were derived using basic calculus on the non-linear equation (Annex I).

2.3.1 Post-Impoundment Annual CH_4 Diffusive Emission Model

The current best model to predict the CH_4 diffusive emissions uses the age of the reservoir; mean annual temperature; and littoral area, as show in Table 2. The statistical details and importance of variables can be found in Annex I.

Table 2: Predicting variables of the gross annual CH_4 diffusive emission model and their effect on CH_4, arrow pointing up meaning positive effect of the variable on the emission and arrow pointing down meaning negative effect of the variable on the emission.

Variables in the model	Direction of the variable effect
Age of the reservoir	↓
Mean annual temperature (°C)	↑
Littoral area (%)	↑

Solving the resulting regression equation for reservoirs of different ages shows that CH_4 diffusive emissions are not constant through but instead decline slowly but steadily over time. An example of the declining CH_4 emissions with age is shown in Figure 5.

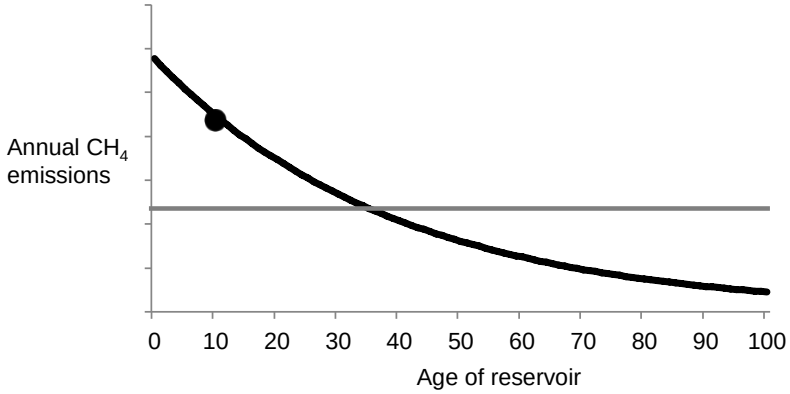

Figure 5: Example of change in annual CH_4 diffusive emissions in time (years) for a reservoir. Black dot is representing the annual CH_4 emissions for the actual age of a reservoir and the grey line represents the integrated emission on lifetime (100 years)

2.3.1.1 CH_4 Bubbling Emission Model

Because of the very low solubility of CH_4 relative to CO_2, CH_4 can reach supersaturation levels that are sufficiently high to initiate the creation of bubbles within the sediments. When released from the sediments because of a sudden change in water level, barometric pressure, or simply by buoyancy, CH_4 bubbles can largely bypass any exchange with the surrounding water and be evaded directly to the atmosphere. This phenomenon, termed methane ebullition, is very difficult to quantify because it is highly variable both spatially (Maeck et al. 2013; DelSontro et al. 2015) and temporally (e.g., Mattson et al. 1990). In some systems, CH_4 ebullition constitutes the main transport mechanism to the atmosphere.

The approach to estimating CH_4 emissions through bubbling is analogous to that estimating diffusive fluxes. In short, all reservoir-wide CH_4 bubbling estimates in peer-reviewed literature were collected and standardized to annual values from which a predictive statistical model was developed. Similar to the approach for CH_4 diffusive emissions, the selected model to best predict the CH_4 bubbling also has the general form of a logarithmic equation (refer to section 2.3 Descriptions of the Semi-empirical Models) and uses the cumulative global horizontal radiance and littoral area as predictor variables (

Table 3). Because of the fewer data points available for bubbling emissions from reservoirs (n=46), and because of the wide confidence limits of the model, estimates of CH_4 ebullition remain relatively poorly constrained but are globally applicable. Statistical details and importance of variables for this model can be found in Annex I.

Table 3: Predictor variables of the annual CH_4 bubbling emission model and their effect on CH_4, arrow pointing up meaning positive effect of the variable on the emission.

Variables in the model	Direction of the variable effect
Cumulative global horizontal radiance (kWh/m²/period)[1]	↑
Littoral area (%)	↑

[1] Please check Annex III for Cumulative global horizontal calculation

2.3.1.2 CH_4 Degassing Emission Model

Contrary to lakes, reservoir outflows can draw water from various depths of the water column, depending on the particular configuration of a dam. Because deep and anoxic water layers can sustain high dissolved CH_4 concentrations, one pathway of CH_4 emissions unique to reservoirs results from the sudden liberation of CH_4-rich water from the deeper layers to the outflowing river when the water is released from low-level outlets. Excess CH_4 is then released to the atmosphere by the sudden pressure drop after the water leaves the outlet, a phenomenon known as reservoir degassing, in what is considered downstream emissions. To estimate this emission pathway correctly, we need to determine first if the intake of the reservoir is in the deepest layer. If so, the following model is applied. If we only have surface intake water, we can omit the degassing pathway. The approach to predicting this source of emissions consisted in developing statistical inference models based on literature-extracted estimates of CH_4 degassing. In this particular case, available measurements of differences in CH_4 concentrations between immediately upstream and immediately downstream of the dam were used. The accuracy of such estimates is difficult to ascertain because there is no generally accepted operational definitions of upstream and downstream locations as it depends on sampling safety and security issues. Nevertheless, a statistically sound model to predict the CH_4 degassing was developed based on the positive relationship between the upstream and downstream concentration difference (as reported in the published literature) with the water residence time and the post-impoundment annual CH_4 diffusive emission predicted by the model described in section 2.3.1 Post-Impoundment Annual CH_4 Diffusive Emission Model. Given the relative strength of this relationship (r^2>0.68), it provides objective and widely applicable method for predicting degassing emissions. Statistical details and importance of variables for this model can be found in Annex I.

2.3.1.3 Relative Contribution to CH_4 Emission

The total post-impoundment CH_4 emissions are then calculated as the sum of the three different types of CH_4 emissions: Post-impoundment CH_4 diffusive emission; CH_4 bubbling emission; and CH_4 degassing emission. To better understand the relative contribution of each of those CH_4 emission pathways, a percent (%) of the total net post-impoundment CH_4 emissions is presented in G-res. The net CH_4 emissions are then calculated by subtracting the pre-impoundment CH_4 balance of the reservoir landscape.

2.3.2 Predicted Gross Annual CO_2 Emission Model

In the case of CO_2, the best selected predictive model (from the elastic net procedure) to predict the CO_2 flux uses the age of the reservoir, mean annual temperature, P concentration, reservoir area and reservoir surface soil carbon content, as shown in Table 4.

Table 4: Predicting variables of the Gross annual CO_2 emission model and their effect on CO_2, arrow pointing up meaning positive effect of the variable on the emission and arrow pointing down meaning negative effect of the variable on the emission.

Variables in the model	Direction of the variable effect
Age of the reservoir	↓
Mean annual temperature (°C)	↑
P concentration (µg L^{-1})	↑
Reservoir area (km^2)	↑
Reservoir surface soil carbon content (kgC m^{-2})	↑

For CO_2 emissions prediction, the tendency to decline with age is much steeper at first, and rapidly stabilizes to a new equilibrium (Figure 7). It is important to note (as was the case for CH_4), that the rapid decline of emissions after impoundment is not imposed by the modelling approach. Rather, it is the empirical data that dictates the shape of the resulting predictive equation. Statistical details and importance of variables for this model can be found in Annex I.

3.1.2 Estimating the CO_2 Emissions Rightfully Attributable to the Reservoir

While the CH_4 emissions occurring at the surface can largely be attributed to the creation of the reservoir (subtracting the CH_4 emissions from the landscape prior to the impoundment), the case of CO_2 emissions is fundamentally different and needs further treatment. A large proportion of the CO_2 emitted from the reservoir is derived from the mineralization of organic carbon (mostly dissolved) originating from the upstream catchment. Some of this organic matter mineralization would therefore occur regardless of the presence of the reservoir. The longer water residence time of a reservoir compared with the river present before impoundment may allow, like any other aquatic system, a greater mineralization within the reservoir (e.g. Dillon and Molot 1997); although it would have occurred further downstream in its original state (Figure 6). Therefore, these reservoir emissions constitute a case of displaced emissions and should be discounted from the reservoir emissions, as they would have occurred in any case, albeit at a different location.

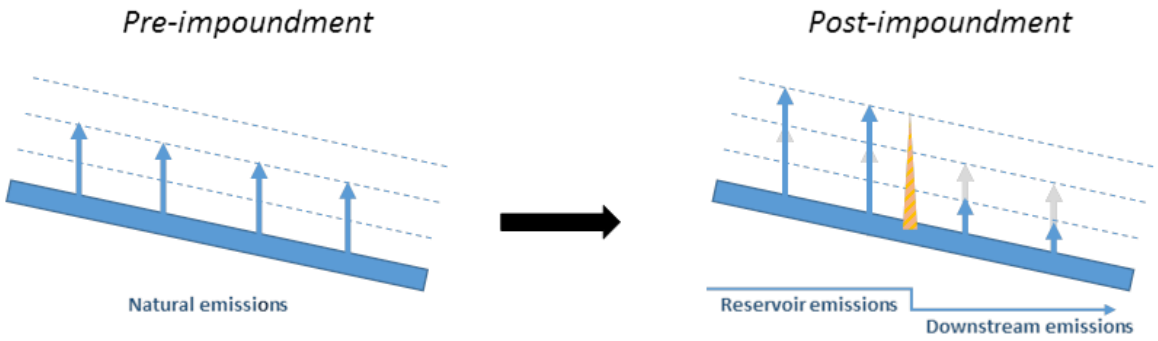

Figure 6: Example of the CO_2 emissions of the river before the impoundment, and the displaced CO_2 emissions after the impoundment of a reservoir

Annual CO_2 Emission Integrated on 100 years Without Natural Baseline

The method used to appropriately consider only emissions attributable to the presence of the reservoir i.e., that would not have occurred if the dam had not been built as discussed below is derived from the models we produced to predict the evolution of gross CO_2 emissions through the lifetime of the reservoir. It can be seen from the shape of the temporal trajectory of CO_2 emission that the initial pulse of CO_2 is stabilizing within the 100 years lifetime of the reservoir (Figure 7). We are thus predicting the integrated emission of the 100 first years after impoundment, but without considering the natural baseline expressed as the emission achieved after 100 years. This can be readily calculated by integrating the model equation from 0 to 100 years using basic calculus and then subtracting the emission at 100 years (Annex III).

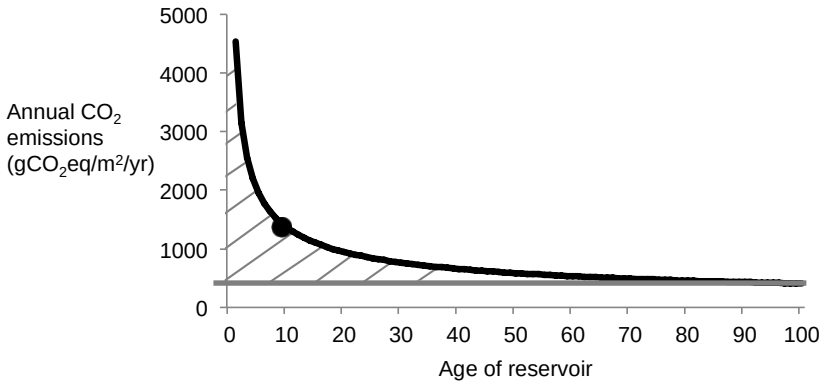

Figure 7: Example of change in annual CO_2 emissions in time (years) for a reservoir. The black dot represents the annual CH_4 emissions for the actual age of a reservoir and the grey hatched area represents the integrated emission on 100 years without the natural baseline

Net Impounded Area

The size of the area that was flooded by the impoundment necessarily needs to be considered in the calculations as a reservoir created by impounding a natural lake and only increasing its surface area slightly will have a much smaller GHG footprint than a large reservoir created by the impoundment of a river. For this reason, all calculations are prorated to the proportion of the reservoir area corresponding to the land flooded by the impoundment.

2.4 Emissions due to Unrelated Anthropogenic Sources

In order to acknowledge that human activities around a reservoir are impacting the water quality and trophic state of the water body (e.g. Matson et al. 1997; Berka et al. 2000; Ahearn et al. 2005; Brett et al. 2005; Jarvie et al. 2010) as well as the amount of GHG emitted by a reservoir affected, Unrelated Anthropogenic Sources (UAS) of GHG emissions were included in the G-res model and can be considered or not in the net GHG footprint. The purpose of this concept is to allocate the anthropogenic sources of nutrients, carbon and direct GHG emissions via inflow water from those occurring directly from inundating the landscape. The logic behind such a separation in G-res tool is twofold:

1) It provides a better distinction of reasons behind increased GHG emissions from reservoirs. While the impoundment of the watercourse may cause increased GHG emissions by changing the controls of the carbon cycle, another reason behind the emissions can be in active land use and sewage release in the catchment. The G-res tool attempts to evaluate the share of UAS that has potential to raise the trophic level by means of nutrient load to the inundated area.
2) Follow-up of the United Nations 1992 Rio Declaration Principle 16 ("Polluter Pays Principle"). According to that principle, the environmentally harmful GHG emissions from the impoundment, caused by other actors in the watershed, should be attributed to any contributing activity.

Changes in the trophic level of a lake (Liikanen et al. 2003; Huttunen et al. 2003; Juutinen et al. 2009) or a reservoir (DelSontro et al. 2010) impacts CH_4 emissions, so by increasing nutrient efflux, various human activities may contribute to CH_4 emissions. An important distinction here is between the catchment "land cover" and "land use". Some land cover types may describe environments without any human intervention such as natural forests and grasslands, whereas some land cover results from management of croplands, pastures, or forestry. The definitions of managed lands may vary in different countries. For example, for the purpose of inclusion in National Greenhouse Gas Inventories, the signatory countries of the UNFCCC and the Kyoto Protocol were allowed to declare all of their forests as managed land or distinguish their natural forests from the managed ones.

In G-res tool, the user can describe the UAS activities in the catchment by providing the annotation of "% of land use intensity" to land cover types by means of "land use intensity". A low % intensity means "mostly non-UAS affected land cover", whilst high % intensity can be used to assign land cover type as a signature of land management. As a result, the G-res tool includes the potential nutrient release from that managed land area (P load used as a land cover specific proxy for all eutrophying nutrients), and estimates the risk of UAS, respectively. The values in the list of land cover/land use specific P loads can be replaced with values appropriate to the system under inspection. Another functionality allows the description of P load from community and industrial sewage. The community sewage load estimate is by default based on Population Equivalent P load (e.g., HELCOM 2014) and characteristics of sewage treatment capacity (if any, section 2.2.7 Other Calculated Information). Industrial sewage load is set to 0 by default. Both values can be given as a bare total P load if known.

The P loads originating from land use and sewage load are summed, and the proportional contribution of the UAS factors to the reservoir's P balance is evaluated. The share of UAS in P concentration in the reservoir that exceeds the expected natural state of the water body (if all human land uses are replaced by natural forest) is assumed to correspond to the respective share of UAS in raised CH_4 emission.

It is recognized that the ratio between the P load and CH_4 is not a mechanistic one, but this assumption is used in the G-res tool CH_4 assessment because eutrophication is known to ultimately increase anoxic conditions in freshwater bodies (e.g., Giles et al 2016). Anoxia, in turn, a prerequisite for CH_4 generation, suppresses CH_4 oxidation (e.g., Huttunen et al. 2003; Juutinen et al. 2009) and has been shown to frequently occur in eutrophied water bodies. Similar observations have been reported from reservoirs with obvious impact from the catchment (e.g., DelSontro et al. 2010). Currently there is no methodology to support the relation of UAS to heterotrophic net CO_2 emission from the reservoir.

The risk of UAS impact on increased CH_4 emissions is evaluated using a simple risk analysis method, *Weighted Sum Model* (WSM*)* (Triantaphyllou et al. 1998). Decision support to the user is given by means of showing the cumulation of various risk indicators: More indicators of UAS - Higher probability of UAS generated CH_4. In the calculation the indicators are assigned weights (*wk*) using a simple Weighted Sum Model method. The method requires that units of indicators (*F*) are the same. That is satisfied by viewing then using the P load estimates for each indicator *k*. The equation of this is then:

WSM = w1*F1 + w2*F2 + … + wk*Fk, where

Wk = Areal ratio * Intensity * P load (Fk)

The *WSM* sum can be used to compare the effects of different variants of input values regarding the UAS factors when the G-res tool is applied in sensitivity analysis of a single project to evaluate different catchment management options. However, the *WSM* risk values between different projects are not directly comparable, because the values in the current version of G-res tool are affected by absolute areas of land use types.

2.5 Construction Module

2.5.1 Scope of assessment

The manufacture, transportation and installation of reservoir infrastructure can lead to emissions of GHG. These emissions are a one-off source of GHG that can be attributed to the services that the reservoir provides.

The construction phase module in G-Res provides an indicative estimate of the construction phase emissions which includes the manufacture of raw materials (the embodied carbon), transportation of materials to, from and around the site, and the energy use from plant used for installation of reservoir infrastructure. Note temporary accommodation and worker movements are not explicitly included, but they can be added by the user in the 'total emissions' assessment option.

As the assessment only attempts to provide an 'order of magnitude' level of accuracy, where the emissions are predicted to be high in comparison to that from the reservoir itself, it is recommended that a more detailed, lifecycle-type assessment be undertaken to fully understand the potential impacts.

2.5.2 Calculation approach

To estimate GHG emissions associated with the construction phase, the consumption of materials, plant and transport associated with the construction of the infrastructure must be known. In some cases, this information will be readily known; however, in other cases, such as early design, this information is not known. The calculation of GHG emissions is based on a simple set of equations that relate the amount of a material, plant, or unit of transport to a GHG emission factor, along the following logic:

GHG Emissions = amount of consumption or activity x emission rate per unit of activity

Material consumption is specified by the user in terms of volume or mass depending on the material in question by the user. Construction plant is specified in terms of energy use from

the construction plant, whether that is direct combustion or electricity use. Finally, construction transport is specified in terms of tonne-kilometres – this is a unit that combined the amount of material being transported over a given distance (e.g., moving 100 tonnes over 2km gives 100t x 2km = 200 tonne-kilometres).

The total CO_2 emissions are calculated based on the inputs of any of the cells regardless of which section has been completed. This means that the user can used some of the activities defined in G-res and add in their own additional activities using the 'Own assessment' option.

2.5.3 Activity data

A set of materials and assets have been included in G-res that allow carbon emissions to be calculated. This requires the user to specify the amount of these materials and assets for the project being assessed.

The models calculate carbon emissions for each material that will be used in the dam project, using known or estimated quantities that are input by the user. They are set up to produce the most accurate results possible with the data available, and as such the options allow for different scenarios.

Option 1 - total emissions

The user can input the total amount of construction emissions if these have previously been calculated and the value is known. For example, a specific assessment may have undertaken as part of an environmental impact assessment or life cycle analysis.

Option 2 - basic assessment

The user can input quantities for the materials most likely to contribute a significant proportion of the construction phase GHG emissions. These categories are earth and rockfill, concrete, and steel.

Emissions are calculated based on values provided for quantities of material and the distance each material travelled to/from site. Emissions from construction plant and transport are then also included based on the input value.

An example calculation is shown below:

GHG = concrete (m^3) x concrete material EF ($kgCO_2/m^3$)
+ mass (tonne) x distance (km) x transport EF ($kgCO_2$/tkm)
+ concrete (m^3) x plant EF ($kgCO_2/m^3$)

This is repeated for each item and the results summed to give the total result.

Option 3 - detailed assessment

As above for option 2, except users input data that provide a greater degree of accuracy. Quantities are input for individual material types under the following categories: Earthworks, Fill, Concrete works, Steelworks, Roads and Bridges, and Equipment. The calculation is worked out on the same basis as the basic assessment methodology (amount of activity multiplied by the appropriate set of emission factors).

2.5.4 Emission Factors

Each unit of activity is combined with an emissions factor as set out in the equation above. Emission Factors have all been sourced from the following references unless none were available, in which case they have been calculated.

Materials

- *The Inventory of Carbon and Energy (ICE) V2.0, The University of Bath, 2011*

The ICE V2 database is an embodied carbon and energy database for construction materials, with over 200 materials broken down in to around 30 subcategories of major building materials. The energy data provides the energy required to produce the material, which gives rise to the embodied carbon emissions.

- *The World Bank Carbon Emissions Estimating Tool (CEET), 2014*

The World Bank published the CEET to estimate GHG emissions from non-financial departments. It is consistent with the GHG Protocol standard and builds on the Carbon Tool (Bilan Carbone) developed by Agencie de Developpement (AFD). It includes emission factors from the United Nations Intergovernmental Panel on Climate Change (IPCC) and the International Energy Agency (IEA).

- *The Civil Engineering Standard of Method and Measurement Fourth Edition (CESMM4), 2012*

CESMM4 is the civil engineering standard for the costing of quantities. It incorporates estimates of embodied carbon values for each civil engineering activity.

Construction Transport

- *The Greenhouse Gas (GHG) Protocol*

The GHG Protocol was developed by the World Resource Institute (WRI) and the World Business Council on Sustainable Development (WBCSD) and is a globally recognised standard for carbon accounting. Transport emission factors in the tool assume HGV Rigid vehicles.

Construction Plant

- *The Civil Engineering Standard of Method and Measurement Fourth Edition (CESMM4), 2012*

2.5.6 Custom Emission Factor Calculations

Where an exact emission factor was not available from a referenced source to match the material type used in the dam project, a custom factor was calculated. For example, for the basic assessment it is assumed that earth and rockfill consists of 50 % granular material and 50% rockfill. An exact emissions factor is not currently available to account for this mix, so an average was calculated from the ICE V2 emissions factor for aggregate material, and the AFD emissions factor for quarry stones.

Custom emission factors for materials are listed in Table 5 below. A full set of the emission factors by the user are presented in Annex X Emission factors for power equipment have been calculated. Power generation equipment includes the power housing and switchyard. Power connection consists of steel cabling, concrete, and conductors.

Power generation

For the power generation equipment, data from Flury and Frischknecht (2012) have been used. In this study, the specific quantity of steel in generating plant is stated as 0.06g/kWh over an 80-year lifetime. This is based on a 95MW plant generating 190GWh per year. Rationalising this to 1MW gives 18 tonnes of steel per MW capacity. This is highly indicative and the value for any given project is likely to be different.

This is then multiplied by the relevant emission factors to calculate the equivalent emissions of CO_2.

Power connection

This element reflects the transmission line equipment and towers required to connect a hydropower plant to the transmission network. This calculation is based on a per kilometre rate and the line voltage. The power connection equipment consists of a mix of transmission towers, conductor, and tower foundations. Quantities of the raw materials – steel and concrete- that make up these components were established, and emission factors from ICE V2 applied to calculate a rate of $kgCO_2$/km. The assumptions for each are presented in the Annex X.

3. Net Predicted Annual Emission

3.1 Reservoir GHG Emissions

To calculate the net GHG emissions from the reservoir, first all the sources of post-impoundment emissions are summed:

- CO_2 emissions
- CH_4 emissions:
  - CH_4 diffusive flux
  - CH_4 bubbling flux
  - CH_4 degassing (only if water intake is below the thermocline)

The post-impoundment emissions are expressed in the G-res as areal emissions ($gCO_2e/m^2/yr$) and as reservoir wide emissions (tCO_2e/yr) merged as GHG emissions but also separately as CO_2 and CH_4. A global warming potential for 100 yrs (GWP100) of 34 was used to obtain CH_4 emissions as CO_2e (IPCC 2013, Annex III).

From this, the emissions that can be observed as emissions at the surface of the reservoir, but that are not attributable to the creation of the reservoir are subtracted:

- Pre-Impoundment emissions representing the emissions balance from the landscape before the impoundment of the reservoir (CH_4 and CO_2 emissions).
- The emission due to the unrelated anthropogenic sources (CH_4 emissions only, optional allocation).

This then results in the estimated net GHG emissions from the reservoir itself.

3.1.1 Distribution within Worldwide Emissions from Reservoir and of Each CH_4 Fraction

The percentile of net GHG emissions expresses the net emissions of the assessed reservoir in comparison to the net GHG emissions of other reservoirs which have been quantified by IHA (note, this does not include other users' reservoirs).

The percentile of each fraction of CH_4 enables a better understanding of what type of CH_4 emissions (diffusive, degassing and bubbling) contribute the most to the net emissions.

Those nearer the 95th percentile have relatively greater emissions than those nearer 5th percentile for example.

3.1.2 95% Confidence Interval of Net GHG Footprint

Each of the emission pathways have their own uncertainty, coming for the empirical models that were developed. To determine the uncertainty of the sum of the 4 pathways, we used the RMSE (Root Mean Square Error) of each model along with the number of observation (n) to determine each of their 95% confidence interval. The 4 pathways are then randomly selected from their normal Gaussian distribution 1000 time (using the Box-Muller algorithm) and summed up together as 1000 Reservoir GHG emissions. The distribution of the 1000 randomly predicted Reservoir GHG emissions is then used to determine the 95% confidence interval of this newly created distribution.

3.2 Total GHG Emissions

Finally, the net GHG Footprint of CH_4 and CO_2 value is evaluated as:

> **Net GHG Footprint = [Post-impoundment GHG balance of the reservoir] – [Pre-impoundment GHG balance of the reservoir area before its introduction] – [Emissions from the reservoir due to unrelated anthropogenic sources (optional allocation] + [GHG due to the construction of the reservoir(optional)]**

The novelty of this model is to integrate not only gross GHG flux to predict the role of a reservoir in atmospheric GHG, but to consider the natural situation before the impoundment. Furthermore, we also consider in this model the strong influence of the aging of the reservoir by using integrated emissions instead of age specific emissions. We can allocate, if desired, the emissions due to UAS of the CH4 estimated in gross emissions and finally add the estimated GHG emissions attributed to the construction phase.

For a better use of the final GHG footprint, the numbers are also presented as:

- **Emissions per m² of reservoir** in $gCO_2e/m^2/yr$
- **Total Reservoir Emissions per year** in tCO_2e /yr
- **Total Lifetime Emissions** in tCO_2e

4. Allocation Module

4.1 Approach

The net annual GHG footprint for a reservoir is allocated to the various reservoir services. Reservoirs provide a range of different economic, social, and environmental services; these include:

- Direct services: power; irrigation; water supply; flood control; transport; commercial fishing; recreation; and environmental services.
- Indirect services: energy; food and water security which enable growth; drought mitigation; and further business opportunities.

The following eight direct services have been included for allocation[1].

1. Flood control
2. Fisheries
3. Irrigation
4. Navigation
5. Environmental flow
6. Recreation
7. Water supply
8. Hydroelectricity

There are several different allocation approaches that have been identified and are set out in Table 6 below, these are:

- Allocation based on relative economic benefit of the services. This approach requires estimating the economic benefit of each service. Zhao and Liu (2015) advocate this approach.
- Allocation based on physical parameters, such as volumetric use or consumption of water, required head or reservoir level, required regulation capacity, required reservoir area. EDF has developed an approach based on allocation of reservoir volume (EDF 2014) and Hakkan et al. (2016) advocate this approach.
- Allocation based on operational regime or hierarchy of services. Many multi-use reservoirs have a rule-based approach to operating the reservoir. In some countries, there is an explicit operating hierarchy to maximise the benefits of a specific service. These operating rules inform operators on water allocation between services where there is a conflict of interest. Hakkan et al. (2016) test this approach in a forthcoming paper.

[1] Refer to EDF (2015), Rodrigues et al. (2006), World Bank Group (2014), Mott MacDonald (2010), Liden & Lyon (2014), Grey & Sadoff (2007), Morimoto & Hope (2012).

Table 6: Different allocation approaches

Approach	Principle	Inclusivity	Implementation
Economic	GHG emissions are allocated based on relative economic benefit provided by the service. In principle, we consider this approach to be most conceptually robust, as decision making is normally based on the economic merits of a project which caused the resultant GHG emissions.	This approach should be possible for all reservoirs. We currently have devised simple methods of including the four most common services.	This approach is the most data intensive, however we have developed a simplified method which we believe is a robust and implementable tier 1 solution.
Volumetric	Allocation based on the changes in volume of water of the reservoir required to fulfil the service. The main conceptual issue is that water is consumed by some services (irrigation) and not by others where the water is only moved from the reservoir.	There are difficulties in including flood control, recreation, and commercial fishing within this approach.	Data requirements of water use over long periods of time may be available to operators.
Operating regime	Approach based on the hierarchy of services in the operating regime. The principle encounters issues for some reservoirs in which hydropower is a major service, but the operation is dominated by irrigation needs.	Should be able to include all services.	Operating hierarchy should be known to operators.

In G-res, the allocation approach is based on the operating regime of the reservoir. The operating regime should be known by the user and therefore will be the most easily implementable of the identified approaches. We continue the development of the economic based approach due to its conceptual robustness; however, at this stage it requires further development.

The operating regime approach allocates GHG emissions based on the operational prioritisation of the services. Operating regimes are informed either by explicit prioritisation or by Operating Rule Curves (ORC). Explicit prioritisation is in place in some countries such as India (Government of India – Ministry of Water Resources), Turkey (Sorman 2013) and Pakistan. The prioritisation ranks the services in order of importance. Some services impose an operational constraint (such as minimum level) but are not ranked in the hierarchy.

ORCs are derived using sophisticated multi-objective optimisation techniques which prescribe a target reservoir level at specific times over the year as a guideline for operators. Operators will therefore release or store water to achieve the level prescribed by the ORC depending on the circumstances at the time. Therefore, the operational prioritisation of the

services changes over time and so the length of time a service is prioritised can be used for allocation.

To implement the operating regime approach, the user must identify the importance, or primacy, of each service. Identifying the primacy is performed using the criteria set out in Table 7 below.

Table 7: Definitions of primary, secondary, and tertiary services

Importance	Explicit Prioritisation	Operating Rule Curve
Primary	Ranked 1 to 3 in operational hierarchy.	Operating rules are designed to maximise these services benefit for part or all of the year.
Secondary	Ranked lower than 3 in operational hierarchy, or places constraints on operation.	The service places operational constraints on the operating level of the reservoir for part or the whole of the year.
Tertiary	Provides benefits but does not alter the operation of the reservoir.	The service provides benefits but has little impact on the operation of the reservoir.

Finally, the GHG emissions need to be apportioned to each of the services. The apportionment follows a simple set of rules:

1. Apportionment for total GHG emissions is as follows: 80% for primary, 15% for secondary and 5% for tertiary. If there is more than one service in each level, the apportionment for that level is split equally between them.
2. There is a maximum of three services in each level. This means a lower-level service will never have a greater apportionment than a higher level service.
3. Where there are no tertiary services, the apportionment (5%) is split between the secondary services. If there is no secondary service, the apportionment (20%) is split between the primary services.

5. Conclusion

Past assessments of GHG emissions from reservoirs have often used simple premises and estimated the GHG footprint by extrapolation from average measured values. In contrast, the G-res modeling framework developed here attempts to consider the environmental setting of individual reservoirs drawing upon globally consistent information layers about its climate, shape, catchment and reservoir properties, hydrological regime, and a suite of other variables to better predict the expected GHG response of reservoirs and how it changes over the course of its lifetime.

A unique feature of the G-res is to estimate the GHG footprint that most closely reflects 'what the atmosphere sees' following the conversion of a landscape to a reservoir. Our approach quantitatively introduces the concept of displaced emissions, where some natural emissions that would have occurred regardless of the presence of the network are displaced at the surface of the reservoir. Our model also integrates the GHG balance of the landscape prior to impoundment and distinguishes the GHG contribution of four emission pathways of carbonic GHGs: CO_2 diffusive emissions as well as diffusive, bubbling, and degassing CH_4 emissions.

G-res provides the option to estimate the portion of the emissions associated with human activities within the reservoir's catchment (known as emissions from Unrelated Anthropogenic Sources, UAS). In addition to predicting emissions from the reservoir itself, the modelling framework includes emissions associated with the construction phase of the dam as well as a module allocating the net GHG footprint to the different services of the reservoir such as flood control, irrigation, and hydroelectricity generation.

The impetus for the development of the G-res tool was to facilitate the estimation of the GHG footprint of the societally important infrastructure that freshwater reservoirs constitute. The G-res tool can be used by stakeholders (hydropower companies, consultants, regulatory agencies) to evaluate, with some basic scientific knowledge, the net GHG footprint for a specific reservoir (existing or planned) or for a collection of reservoirs. Despite its unique and advanced features, the G-res modelling framework presented here necessarily carries the limitations associated with the current state of reservoir science and of the data used in its development. For example, cascading systems, where one reservoir receives water from one or multiple reservoirs upstream (design often used in hydropower generation reservoir), are not directly integrated in the current version for lack of published assessment of their GHG behavior. Users should therefore be careful when applying G-res tool in such situations. Similarly, our model currently evaluates only carbonic GHG emissions and does not consider N_2O emissions. The few reservoir N_2O measurements available suggest that it represents only a small fraction of emissions in most reservoirs (Deemer et al 2016). In this context, the G-res should be viewed largely as a warning tool, to be used to determine if the emissions potential of a reservoir is likely important or not. Further fieldwork and assessment is always encouraged in case of high predicted emissions.

6. Bibliographic References

Ahearn DS, Sheibley RS, Dahlgren RA, Anderson,M, Johnson J & Tate KW. 2005. Land use and land cover influenece on water quality in the last free-flowing river draining the western Sierra Nevada, Califormia. *Journal of Hydrology* 313: 234-247.

Bakken H et al. 2016. Allocation of water consumption in multipurpose reservoirs. *Water Policy Uncorrected Proof* 1-17. IWA Publishing 2016. doi:10.2166/wp.2016.009.

Barros N, Cole JJ, Tranvik LJ, Prairie YT, Bastviken D, Huszar VLM, del Giorgio PA and Roland F. 2011. Carbon emission from hydroelectric reservoirs linked to reservoir age and latitude. *Nature Geoscience* 4: 593–596.

Bastviken D, Tranvik LJ,. Downing JA, Crill PM, and Enrich-Prast A. 2011. Freshwater Methane Emissions Offset the Continental Carbon Sink. *Science* 331: 50–50.

Berka C, Schreier H, and Hall K. 2000. Linkin water quality with agricultural intensification in rural watershed. *Water, Air, and Soil Pollution* 127: 389-401.

Borges AV, Morana C, Bouillon S, Servais P, Descy JP and Darchambeau F. 2014. Carbon cycling of Lake Kivu (East Africa): Net autotrophy in the epilimnion and emission of CO2 to the atmosphere sustained by geogenic inputs. *PLOS ONE* 9: 10.

Brett MT, Arhonditsis GB, Mueller SE, Hartley DM, Frodge JD, and Funke DE 2005. Non-point-source impacts on stream nutrient concentrations along a forest to urban gradient. *Environmental Management* 35: 330-342.

Cailleaud E, Serça D and Guérin F. 2015. Cycles du carbone et de l'azote et émissions de gaz à eet de serre (CH4, CO2 et N2O) du lac de barrage de Petit Saut et du fleuve Sinnamary en aval du barrage (Guyane Française) (PhD dissertation). Université de Toulouse, Toulouse, France.

CIESIN (Center for International Earth Science Information Network), Columbia University; and Centro Internacional de Agricultura Tropical (CIAT). 2020. Gridded Population of the World Version 4 (GPWv4): Population Density Grids. Palisades, NY: *Socioeconomic Data and Applications Center (SEDAC), Columbia University.* Available online at http://sedac.ciesin.columbia.edu/gpw.

Cole J, Prairie YT, Caraco N, Mcdowell W, Tranvik L, Striegl R, Duarte C, Kortelainen P, Downing J, Middelburg J and Melack J. 2007. Plumbing the global carbon cycle: Integrating inland waters into the terrestrial carbon budget. *Ecosystems* 10: 171–184.

DelSontro T, Mcginnis DF, Sobek S, Ostrovsky I and Wehrli B. 2010. Extreme methane emissions from a swiss hydropower Reservoir: Contribution from bubbling sediments. *Environmental Science and Technology*, *44*(7), 2419–2425. doi:10.1021/es9031369

Dillon P, and Molot L. 1997. Dissolved organic and inorganic carbon mass balances in central Ontario lakes. *Biogeochemistry* 36: 29–42.

EDF. 2014. Water consumption allocation in a multi-usage scenario.

EDF (Branche, E.). 2015. Multipurpose water uses of hydropower reservoirs. Sharing the water uses of multipurpose hydropower reservoirs: the SHARE concept. Main document – Final.

ESA-CCI. 2014-2017. The Land Cover CCI Climate Research Data Package (CRDP). European Space Agency (ESA) – Climate Change Initiative (CCI) - Land Cover project. Available online at http://maps.elie.ucl.ac.be/CCI/viewer/download.php.

FAO/IIASA/ISRIC/ISSCAS/JRC. 2012. Harmonized World Soil Database (version 1.2). FAO, Rome, Italy and IIASA, Laxenburg, Austria. Available online at http://webarchive.iiasa.ac.at/Research/LUC/External-World-soil-database/HTML/.

Feteke BM et al. 2000. Global Composite Runoff Fields Based on Observed River Discharge and Simulated Water Balances. Complex Systems Research Center, University of New Hampshire. *UNH-GRDC Composite Runoff Fields v1.0*. Available online at http://www.grdc.sr.unh.edu/.

Flury F and Frischknecht R. 2012. Life Cycle Inventories of Hydroelectric Power Generation. *ESU-services Ltd., fair consulting in sustainability*. Available online at http://treeze.ch/fileadmin/user_upload/downloads/Publications/Case_Studies/Energy/flury-2012-hydroelectric-power-generation.pdf

Gagnon L, Bélanger C and Uchiyama Y. 2002. Life-cycle assessment of electricity generation options: The status of research in year 2001. *Energy Policy* 30: 1267–1278.

GHG Protocol Emission Factors from Cross-Sector Tools. 2014.

Giles DC, Isles PDF, Manley T, Xu Y, Druschel GK and Schroth AW. 2016. The mobility of phosphorus, iron, and manganese through the sediemtn-water continuum of shallow eutrophic freshwater lake under stratified and mixed water-column conditions. *Biogeochemistry* 127: 15-34.

GLOBE Task Team and others (Hastings, David A., Paula K. Dunbar, Gerald M. Elphingstone, Mark Bootz, Hiroshi Murakami, Hiroshi Maruyama, Hiroshi Masaharu, Peter Holland, John Payne, Nevin A. Bryant, Thomas L. Logan, J.-P. Muller, Gunter Schreier, and John S. MacDonald), eds. 1999. The Global Land One-kilometer Base Elevation (GLOBE) Digital Elevation Model, Version 1.0. National Oceanic and Atmospheric Administration, National Geophysical Data Center, 325 Broadway, Boulder, Colorado 80305-3328, U.S.A. Digital data base on the World Wide Web (URL: http://www.ngdc.noaa.gov/mgg/topo/globe.html) and CD-ROMs.

Gorham, E. & Boyce, F. 1989. Influence of lake surface area and depth upon thermal stratification and the depth of the summer thermocline. *Journal of Great Lakes Research* 15: 233–245.

Government of India – Ministry of Water Resources (undated). State Water Policies and the National Water Policy for water management practices. Available online at http://wrmin.nic.in/writereaddata/linkimages/anu29668628373.pdf.

Grey and Sadoff. 2007. Sink or Swim? Water security for growth and development. *Water Policy* 9 545-571.

Guérin F, Abril G, de Junet A and Bonnet MP. 2008. Anaerobic decomposition of tropical soils and plant material: Implication for the CO2 and CH4 budget of the Petit Saut Reservoir. *Applied Geochemistry* 23: 2272–2283.

Heathcote AJ, del Giorgio PA and Prairie YT. 2015. Predicting bathymetric features of lakes from the topography of their surrounding landscape. *Canadian Journal of Fisheries and Aquatic Sciences* 72: 643–650.

HELCOM 2014. OSPAR RID Guidelines 4.2. DRAFT4 UPDATED. Riverine Inputs and Direct Discharges Monitoring Programme (RID). https://portal.helcom.fi/meetings/PLC-6%206-2014-131/MeetingDocuments (Linked February 26, 2016).

Hengl, T., Mendes de Jesus, J., Heuvelink, G. B.M., Ruiperez Gonzalez, M., Kilibarda, M. et al. (2017) SoilGrids250m: global gridded soil information based on Machine Learning. PLoS ONE 12(2): e0169748. doi:10.1371/journal.pone.0169748.

Hijmans RJ, Cameron SE, Parra JL, Jones PG and Jarvis A. 2005. Very high resolution interpolated climate surfaces for global land areas. *International Journal of Climatology* 25: 1965-1978. Available online at www.worldclim.org.

Huttunen JT, Alm J, Liikanen A, et al. 2003. Fluxes of methane, carbon dioxide and nitrous oxide in boreal lakes and potential anthropogenic effects on the aquatic greenhouse gas emissions. *Chemosphere* 52 (3): 609-621.

Huttunen JT, Alm J, Saarijarvi E, et al. 2003. Contribution of winter to the annual CH4 emission from a eutrophied boreal lake. *Chemosphere* 50(2): 247-250.

IAEA Working Materials Document 1995. 1995. Assessment of Greenhouse Gas Emissions from the Full Energy Chain .~r Nuclear" Power and Other Energv Sources. IAEA Advisory Group Meeting, Vienna, Austria, 26-28 September.

IAEA Working Materials Document 1996. 1996. Assessment of Greenhouse Gas Emissions from the Full Energy Chain for Hydropower, Nuclear" Power and Other Energy Sources. IAEA Advisory Group Meeting, jointly organized by Hydro-Qu6bec, Hydro-Qu6bec Headquarters, Montreal (Canada), 12-14 March. Juutinen S. 2003. Major implication of the littoral zone for methane release from boreal lakes. Global Biogeochemical Cycles 17: 1–11.

Imboden , DM. 1973. "Limnologische Transport- und Nahrstoffmodelle." Schweiz. Z. Hydra!., vol. 35, p. 29-68.

Inglett KS, Inglett PW, Reddy KR and Osborne TZ. 2012. Temperature sensitivity of greenhouse gas production in wetland soils of different vegetation. *Biogeochemistry* 108: 77–90.

Inventory of Carbon and Energy, University of Bath. 2011.

IPCC. 2006. 2006 IPCC Guidelines for National Greenhouse Gas Inventories, Prepared by the National Greenhouse Gas Inventories Programme, Eggleston H.S., Buendia L., Miwa K., Ngara T. and Tanabe K. (eds). Published: *IGES*, Japan.

IPCC. 2011. IPCC Special Report on Renewable Energy Sources and Climate Change Mitigation. Prepared by Working Group III of the Intergovernmental Panel on Climate Change [O. Edenhofer, R. Pichs-Madruga, Y. Sokona, K. Seyboth, P. Matschoss, S. Kadner, T. Zwickel, P. Eickemeier, G. Hansen, S. Schlömer, C. von Stechow (eds)]. *Cambridge University Press*, Cambridge, United Kingdom and New York, NY, USA.

IPCC. 2014. 2013 Supplement to the 2006 IPCC Guidelines for National Greenhouse Gas Inventories: Wetlands, Hiraishi, T., Krug, T., Tanabe, K., Srivastava, N., Baasansuren, J., Fukuda, M. and Troxler, T.G. (eds). Published: IPCC, SwitzerlandJørgensen, S.E., Halling-Sørenen, B., Nielsen, S.N., 1996. *Handbook of Environmental and Ecological Modeling. Lewis Publishers, Boca Raton*. 672 pp.

Jarvie HP, Withers PJA, Bowes MJ. Palmer-Felgate EJ, Harper DM, Wasiak K, Hodginson RA, Bates A, Stoate C, Neal M, Wickham HD, Harman SA and Armstrong LK. 2010. Streamwater phosphorus and nitrogen across a gradient in rural-agricultural land use intensity. *Agriculture, Ecosystems and Environment* 135: 239-252.

Juutinen S, Rantakari M, Kortelainen P, Huttunen JT, Larmola T, Alm J, Silvola J and Martikainen PJ 2009. Methane dynamics in different boreal lake types. *Biogeosciences* 6(2): 209-223.

Kim Y, Roulet NT, Li C, Frolking S, Strachan IB, Peng C, Teodoru CR, Prairie YT and Tremblay A. 2016. Simulating carbon dioxide exchange in boreal ecosystems flooded by reservoirs. *Ecological Modelling* 327: 1–17.

Larsen, DP and Mercier, HT. 1976. Phosphorus retention capacity of lakes. *Journal of the Fisheries Research Board of Canada 33:1742-1750*

Lehner B, R-Liermann C, Revenga C, Vörösmarty C, Fekete B, Crouzet P and Döll P. 2008. High resolution mapping of the world's reservoirs and dams for sustainable river flow management. *Frontiers in Ecology and the Environment. GWSP Digital Water Atlas. Map 81: GRanD Database (V1.0).* Available online at http://atlas.gwsp.org.

Liikanen A, Murtoniemi T, Tanskanen H, Väisänen T and Martikainen P. 2002. Effects of temperature and oxygen availability on greenhouse gas and nutrient dynamics in sediment of a eutrophic mid-boreal lake. *Biogeochemistry* 59: 269–286.

Liikanen A, Huttunen JT, Murtoniemi T et al. 2003. Spatial and seasonal variation in greenhouse gas and nutrient dynamics and their interactions in the sediments of a boreal eutrophic lake. *Biogeochemistry* 65 (1): 83-103.

Liden R and Lyon K. 2014. The hydropower sustainability assessment protocol for use by World Bank clients : lessons learned and recommendations. Water partnership program (WPP) *Water papers. Washington, DC: World Bank Group*.

Maeck A, DelSontro T, McGinnis DF, Fischer H, Flury S, Schmidt M, Fietzek P and Lorke A.

2013. Sediment Trapping by Dams Creates Methane Emission Hot Spots. *Environ. Sci. Technol* 47: 8130–3137.

Matson PA, Parton WJ, Power AG and Swift MJ. 1997. Agricultural intensification and ecosystem properties. *Science* 277: 504-509.

Mott MacDonald. 2010. Gibe III Hydropower Project – Final EFTA Study Report.

Morimoto & Hope. 2012. Applying a cost-benefit analysis model to the Three Gorges project in China. *Impact Assessment and Project Appraisal* Vol. 22 / Iss. 3 2004.

NASA Surface meteorology and Solar Energy (SSE) Release 6.0 Data Set (Jan 2008) 22-year Monthly & Annual Average (July 1983 - June 2005). Available online at http://eosweb.larc.nasa.gov/sse/

Pan Y, Birdsey RA, Fang J, et al. 2011. A Large and Persistent Carbon Sink in the World's Forests. *Science* 333 (6045): 988-993. DOI: 10.1126/science.1201609.

Prairie Y. and Kalff J. 1986. Empirical models of phosphorus in streams and lakes. Thesis, McGill University.

Rasilo T, Prairie YT and del Giorgio PA. 2014. Large-scale patterns in summer diffusive CH4 fluxes across boreal lakes, and contribution to diffusive C emissions. *Global Change Biology* 1: 1–16.

Raymon PA, Hartmann J, Lauerwald R, Sobek S, McDonald C, Hoover M, Butman D, Striegl R., Mayorga E, Humborg C, Kortelainen P, Dürr H, Meybeck M, Ciais P and Guth P. 2013. Global carbon dioxide emissions from inland waters. *Nature* 503: 355–359.

Read J, Hamilton D, Jones I, Muraoka K, Winslow L, Kroiss R and Gaiser E. 2011. Derivation of lake mixing and stratification indices from high-resolution lake buoy data. *Environmental Modelling & Software*, *26*, 1325–1336.

Rodrigues et al. 2006. Water Evaluation and Planning (WEAP). *Small Reservoirs Toolkit* .

Rubel F and Kottek M. 2010. Observed and projected climate shifts 1901-2100 depicted by world maps of the Köppen-Geiger climate classification. *Meteorol.* Z., 19, 135-141. DOI: 10.1127/0941-2948/2010/0430. Available online at http://koeppen-geiger.vu-wien.ac.at/shifts.htm.

Sorman, A.Ü. 2013. Presentation at Workshop on allocation and water transaction; Ankara, 15-17 April 2013 organized by the State Hydraulic Works (DSI) in Turkish.

Teodoru CR, Bastien J, Bonneville MC, del Giorgio PA., Demarty M, Garneau M, Hélie JF, Pelletier L, Prairie YT, Roulet NT, Strachan IB and Tremblay A. 2012. The net carbon footprint of a newly created boreal hydroelectric reservoir. *Global Biogeochemical Cycles* 26: 1–14.

Tranvik L, Downing J, Cotner J, Loiselle S, Striegl R, Ballatore T, Dillon P, Finlay K, Fortino K, Knoll L, Kortelainen P, Kutser T, Larsen S, Laurion I, Leech D, McCallister S, McKnight D, Melack J, Overholt E, Porter J, Sobek S, Tremblay A, Vanni M, Verschoor A, Wachenfeldt E and Weyhenmeyer G. 2009. Lakes and reservoirs as regulators of carbon cycling and climate. *Limnology and oceanography* 54: 2298–2314.

Triantaphyllou B, Shu S, Nieto Sanchez and Ray T. 1998. Multi-criteria Decision Making: An Operations Research Approach. Published in *Encyclopedia of Electrical and Electronics Engineering*, (J. G. Webster, Ed), John Wiley & Sons, New York, NY, Vol. 15, Pg. 175-186.

UN DESA 2018 List of Least Developed Countries (as of March 2018) United Nations Committee for Development Policy Development Policy and Analysis Division Department of Economic and Social Affairs Available online at https://www.un.org/development/desa/

dpad/wp-content/uploads/sites/45/publication/ldc_list.pdf

Vachon D, and Prairie YT. 2013. The ecosystem size and shape dependence of gas transfer velocity versus wind speed relationships in lakes. *Canadian Journal of Fisheries and Aquatic Sciences*, *70*(August), 1757–1764. doi:10.1139/cfjas-2013-0241.

Wetzel R. 2001. Limnology Lake and River Ecosystems. *Elsevier Academic Press*.

Whipple KX, DiBiase RA and Crosby BT. 2013. Bedrock rivers. In: Shroder, J. (Editor in Chief), Wohl, E. (Ed.), *Treatise on Geomorphology. Academic Press, San Diego, CA, vol. 9, Fluvial Geomorphology*, pp. 550–573.

World Bank Carbon Emissions Estimating Tool. 2014. (based on data from Agence Française de Developpement).

World Bank Carbon Emissions Estimating Tool. 2014. (based on data from the International Energy Agency).

World Bank Group (Danilenko et al). 2014. The IBNET Water Supply and Sanitation Blue Book 2014. *The International Benchmarking Network for Water and Sanitation Utilities Databook.*

Yvon-Durocher G, Allen AP, Bastviken D, Conrad R, Gudasz C, St-Pierre A, Thanh-Duc N and del Giorgio PA. 2014. Methane fluxes show consistent temperature dependence across microbial to ecosystem scales. *Nature* 507: 488–491.

Zhao D and Liu J. 2015. A new approach to assessing the water footprint of hydroelectric power based on allocation of water footprints among reservoir ecosystem services. *Physics and Chemistry of the Earth* 79–82, 40–46. doi:10.1016/j.pce.2015.03.005.

7. Annexes

Annex I - Statistical details of empirical models

The literature on almost every component of GHG emissions from aquatic systems, whether natural lakes or reservoirs, consistently shows highly skewed data distribution, with most values concentrated at the low end of the spectrum with a few very high values. This is especially true for highly spatio-temporally variable phenomena such as CH_4 bubbling emissions. Depending on the degree of skewness of the data, the resulting mean value can be much higher than the median value. Which of the mean or median values best represent the "expected" emissions is a matter of perspective and of the particular question being asked. In the context of GHG emissions from reservoirs, the distinction is akin to asking what is the most likely emission for a reservoir of a given configuration *versus* what is the average emission from all reservoirs of comparable configurations. For skewed distributions, the most likely emission for a given reservoir is better represented by the median. However, if one is interested in estimating the total emission from an ensemble of reservoirs with similar configurations, then the mean (in statistical terminology, the expected value of the distribution) would be a more appropriate metric to use. Also note that in such situations, the mean is much more difficult to estimate precisely than the median. This can be illustrated using the data set we collated on system-wide CH_4 bubbling emissions (as C-CH_4 g m^{-2} d^{-1}) from 49 published studies (see section 2.3.1.1 on bubbling for more details).

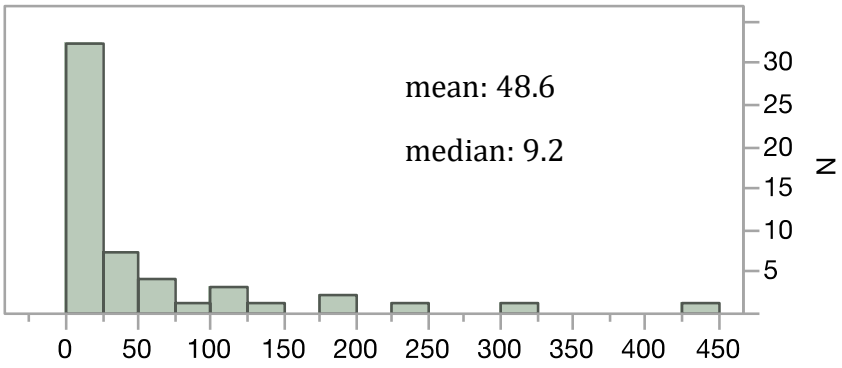

Figure 8: Distribution of system-wide CH_4 bubbling emissions (as C-CH_4 g m^{-2} d^{-1}) from published literature.

In this example, the mean is not only about 5-fold greater than the median, but also much more uncertain. Using bootstrap re-sampling techniques, we can estimate that the confidence interval of the median (90% CI range: 14) will be narrower than that of the mean (90% CI range: 30) by a factor of about 2. This is because the mean is highly sensitive to the few high values and therefore much more susceptible to random sampling fluctuations.

Extrapolating these sample estimates (mean or median) to the global extent of reservoirs of the world requires careful consideration. Beyond the difficulties of estimating the average

in a highly skewed distribution described above, upscaling reservoir emissions from a sample mean assumes that the sampled reservoirs correspond to a representative sample of the global population of reservoirs, not only geographically but also in terms of the GHG emission rates. The extent to which reservoirs that have been sampled may have biased GHG emissions relative to a random sample is difficult to quantify. For this reason, we took an approach that does not rely directly on an unbiased representation of reservoirs in the sample we gleaned from the published literature. Instead, our approach focused on identifying and quantifying the main drivers of emissions from a set of local environmental factors through statistical analyses. Once established, the relationships can be used on a wider data set for which the input variables are known that more closely approaches the population of worldwide reservoirs.

Statistical inference models derived from data that have an inherently skewed distributions are typically fitted after appropriate transformation to make their distribution conform to the underlying assumptions of the analysis. In our case, GHG emissions were all fitted after logarithmic transformation, a very flexible transformation that has the property of better spacing the observations along the X or Y axes, and for making the residual values approximately normal. While this is a standard procedure, it imposes some properties on the predictions from such models that are here briefly considered and that may be important depending on the specific use of the models. In general terms, the statistical models will be of the form:

$$log\ (GHG\ emission)\ =\ f(Temperature,\ Age, other\ drivers\ of\ GHG\ldots)$$

By definition, predictions from such models will be log-normally distributed and simply taking the anti-log of the predicted log(emission) is akin to predicting the median of the distribution and not its mean. This is known in the statistical literature as transformation bias (see Miller 1984). Following the discussion above regarding the appropriateness of the two measures of central tendency depending on the context of application, all our predictions were computed using both the predicted median and predicted mean. This was accomplished using the following multiplicative correction factor (C.F.):

$$C.F. = e^{\sigma_{\hat{\epsilon}}^2/2}$$

where σ^2_{ε} is the residual error variance of the applicable regression model. Generically, prediction of the median are given as

$$\widehat{Median}\ =\ e^{f(Temperature, Age, other\ drivers\ of\ GHG\ldots)}$$

whereas prediction of the mean is given by

$$\widehat{Mean} = C.F. \cdot e^{f(Temperature, Age, other\ drivers\ of\ GHG\ldots)}$$

Statistical equations and details of each model adopted in the G-res tool

CO_2 Diffusive Emissions Integrated on Lifetime (g CO_2e/m²/yr)

$$CO_2\ Diffusive\ Emissions = \left(\left(10^{(1.860 + 0.0332 * Effective\ Temperature\ CO_2 + 0.0799 * log10(Reservoir\ Area) + 0.0155 * Reservoir\ Surface\ Soil\ C\ Content + 0.2263 * log10(TP))} * \frac{100^{(-0.330+1)} - 0.5^{(-0.330+1)}}{(-0.330+1) * (100 - 0.5)} * 0.365 * \frac{44}{12} * \left(1 - \frac{\%\ River\ Area\ Before\ Impoundment}{100}\right)\right) - \left(10^{(1.860 - 0.330 * log10(Age) + 0.0332 * Effective\ Temperature\ CO_2 + 0.0799 * log10(Reservoir\ Area) + 0.0155 * Reservoir\ Surface\ Soil\ C\ Content + 0.2263 * log10(TP))} * \frac{365}{1000} * \frac{44}{12} * \left(1 - \frac{\%River\ Area\ Before\ Impoundment}{100}\right)\right)\right)$$

n=169, R^2=0.36, RMSE= 0.39, Outliers=3

** To obtain the flux in gCO_2e/m²/yr, the result needs to multiply by 44/12 for the transformation from gram of carbon (C) to gram of CO_2 equivalent (CO_2e), to divide by 1000 to transform from miligram (mg) to gram and to multiply by 365 to annualize it. The equation above uses the empirical model equation but also contains the operation necessary to integrate the emissions over 100 years (derived from calculus) and removes the natural emissions estimated as those predicted at 100 years.

Units:
River Area Before impoundment (%)
Effective Temperature CO_2 (°C)
Reservoir Area (km²)
Reservoir Soil Carbon content (kgC/m²)
TP (µg/l)

CH_4 Diffusive Emissions Integrated on 100 yrs (g CO_2e/m²/yr)

$$CH_4\ Diffusive\ Emissions\ Integrated\ on\ 100\ yrs = \frac{10^{\left(0.8032 + 0.4594 * log10\left(\frac{\%\ Littoral\ Area}{100}\right) + 0.04819 * Effective\ Temperature\ CH_4\right)} * (1 - 10^{(-(100 * 0.01419))})}{(100 * 0.01419 * ln(10))} * \frac{365}{1000} * \frac{16}{12} * 34$$

n=160, R^2=0.51, RMSE= 0.52, Outliers=15

** To obtain the flux in gCO_2e/m²/yr, the result needs to multiply by 16/12*34 for the transformation from gram of carbon (C) to gram of CO_2 equivalent (CO_2e), to divide by 1000 to transform from miligram (mg) to gram and to multiply by 365 to annualize it. The equation above uses the empirical model equation but also contains the operation necessary to integrate the emissions over 100 years (derived from calculus). A global

warming potential for 100 yrs (GWP100) of 34 was used to obtain CH_4 emissions as CO_2e (IPCC 2013, Annex III).

Units:
Littoral Area (%)
Effective Temperature CH4 (°C)

CH_4 Bubbling Emissions (g $CO_2e/m^2/yr$)

$$CH_4\ Bubbling\ Emissions = 10^{(-1.3104 + 0.8515 * log10(\frac{\%\ Littoral\ Area}{100}) + 0.05198 * (Reservoir\ Cumulative\ Global\ Horizontal\ Radiance))} * \frac{365}{1000} * \frac{16}{12} * 34$$

n=46, R^2=0.26, RMSE= 0.8, Outliers=3

** To obtain the flux in $gCO_2e/m^2/yr$, the result needs to multiply by 16/12*34 for the transformation from gram of carbon (C) to gram of CO_2 equivalent (CO_2e), to divide by 1000 to transform from milligram (mg) to gram and to multiply by 365 to annualize it. A global warming potential for 100 yrs (GWP100) of 34 was used to obtain CH_4 emissions as CO_2e (IPCC 2013, Annex III).

Units:
Littoral Area (%)
Cumulative GHR (kWh/m^2/period)

CH_4 Degassing Emissions (t C/yr)

$$CH_4\ Degassing\ Emissions = \frac{10^{(-6.9106 + 2.950 * log10(CH4\ Diffusive\ Emissions\ Integrated\ on\ 100\ yrs) + 0.6017 * log10(WRT))} * 1000}{1000000000} * Catchment\ Area * 1000000 * (\frac{Annual\ Runoff\ (mm/yr)}{1000}) * 0.9 * \frac{16}{12} * 34 / Reservoir\ Area\ (km^2)$$

n=38, R^2=0.68, RMSE= 0.81, Outliers=2

** To obtain the flux in $gCO_2e/m^2/yr$, the result needs to multiply by 16/12*34 for the transformation from ton of carbon (C) to gram of CO_2 equivalent (CO_2e) and to divide by the reservoir area (km^2) to bring it as an areal rate. The ton to g and the km^2 to m^2 transformation are equivalent and do not need to be calculated. A global warming potential for 100 yrs (GWP100) of 34 was used to obtain CH_4 emissions as CO_2e (IPCC 2013, Annex III).

Units:
Reservoir Area (km^2)
Annual Runoff (mm/yr)
Catchment Area (km^2)
CH4 diffusive emissions ($gCO_2e/m^2/yr$)
WRT (yr)

Annex II - **Essential Variables for the Prediction of Net GHG Footprint from Reservoirs Using the G-res Tool.**

Catchment area (km^2)
Population in the catchment (persons)
Catchment annual runoff ($mm\ yr^{-1}$)
Land cover % in the catchment area (Croplands, Bares Areas, Wetlands, Forest, Grassland/Shrubland, Permanent Snow/Ice, Settlements, Water Bodies, Drained Peatlands)
Full water supply or mean reservoir area (km^2)
Pre-impoundment land cover % in the reservoir area (Mineral and organic soil; Croplands, Bares Areas, Wetlands, Forest, Grassland/Shrubland, Permanent Snow/Ice, Settlements, Water Bodies, Drained Peatlands)
Country
Climate zone (Reservoir area)
Maximum depth (m) (Dam height could be used as a proxy of this value)
Mean depth (m) (Reservoir area and reservoir volume could be used to calculate this value)
% Littoral area (Maximum and Mean depth could be used to calculate this value)
Thermocline depth (m) (Temperature, Reservoir area and Annual mean wind speed could be used to calculate this value)
Reservoir surface soil carbon content, 0-30 cm ($kgC\ m^{-2}$)
Annual wind speed ($m\ s^{-1}$)
Phosphorus concentration ($\mu g\ L^{-1}$) (Catchment land cover %, Catchment area, Water residence time and Annual runoff speed could be used to calculate this value)
Reservoir mean global horizontal radiance ($kWh\ m^{-2}\ d$)
Water residence time (yr) (Reservoir area, Mean depth, Catchment area and Annual runoff could be used in order to calculate this value)
Monthly mean air temperature (°C)

Annex III **Equation Used in the G-res Tool**

Air Density (kg/m³)

$$Air\ Density\ = \frac{101325}{287.05\ *\ (Mean\ Temperature\ of\ the\ 4\ Warmer\ Months\ + 273.15)}$$

Bottom Temperature (°C)

- If *Mean Temperature of the Colder Month* > 1.4:

$$Bottom\ Temperature\ =\ 0.656 * Mean\ Temperature\ of\ the\ Colder\ Month\ +\ 10.7$$

- If *Mean Temperature of the Colder Month* ≤ 1.4:

$$Bottom\ Temperature\ =\ 0.2345 * Mean\ Temperature\ of\ the\ Colder\ Month\ +\ 10.11$$

Bottom Water Density (kg/m³)

$$Bottom\ Water\ Density = \left[1\ -\ \frac{Bottom\ Temperature\ +\ 288.9414}{508929.2\ *\ (Bottom\ Temperature\ +\ 68.12923) * (Bottom\ Temperature\ -\ 3.9863)^2)}\right] * 1000$$

Surface Temperature (°C)

$$Surface\ Temperature\ =\ Mean\ Temperature\ of\ the\ 4\ Warmer\ Months$$

Surface Water Density (kg/m³)

$$Surface\ Water\ Density = \left[1\ -\ \frac{Surface\ Temperature\ +\ 288.9414}{508929.2\ *\ (Surface\ Temperature\ +\ 68.12923) * (Surface\ Temperature\ -\ 3.9863)^2)}\right] * 1000$$

CD

$$CD\ =\ If\ (Reservoir\ Mean\ Wind\ Speed\ <\ 5\ ;\ 0.001\ ;\ 0.000015\ )$$

Annual Wind Speed at 10m (m/s)

$$Annual\ Wind\ Speed\ at\ 10\ m = Reservoir\ Mean\ Wind\ Speed\ at\ X\ m * \left(1 - \left(\frac{CD^{0.5}}{0.4}\right) * Log10\left(\frac{10}{X}\right)\right)^{-1}$$

** X equal 50m in our database.

Reservoir Volume (km³)

$$Reservoir\ Volume = Reservoir\ Area * (Mean\ Depth/1000)$$

Reservoir Area (km²)

$$Reservoir\ Area = \frac{Reservoir\ Volume}{Mean\ Depth/1000}$$

Mean Depth (m)

$$Mean\ Depth = Volume\ /\ Reservoir\ Area * 1000$$

Thermocline Depth (m)

$$Thermocline\ Depth = 2.0 * \sqrt{\frac{CD * Air\ Density * Annual\ Wind\ Speed\ at\ 10m^2}{9.80665 * (Bottom\ Water\ Density - Surface\ Water\ Density)}} * \sqrt{\sqrt{Reservoir\ Area * 1000000}}$$

**Gorham and Boyce (1989)

In the G-res Tool, if impossible to estimate using Gorham and Boyce (1989), equation from Hanna 1990 used:

$$Thermocline\ Depth = 10^{(0.185 * Log10(:Reservoir\ Area) + 0.842)}$$

Temperature Correction Coefficient CH_4 (To do for Each Month)

$$Temperature\ Correction\ Coefficient\ CH_4 = 10^{(Temperature\ per\ Month * 0.052)}$$

** 0.052 is the slope of the temperature vs CH_4 flux function in our database

** If Temperature per month lower then 4°C, use 4°C

Temperature Correction Coefficient CO_2 (To do for Each Month)

$$Temperature\ Correction\ Coefficient\ CO_2 = 10^{(Temperature\ per\ Month * 0.05)}$$

** 0.05 is the slope of the temperature vs CO_2 flux function in our database

** If Temperature per month lower then 4°C, use 4°C

Effective Temperature CH_4(°C)

$$Effective\ Temperature\ CH_4 = \frac{log10(Average\ (12\ Month\ \ Temperature\ Correction\ Coefficient\ CH_4\ ))}{0.052}$$

** 0.052 is the slope of the temperature vs CH_4 flux function in our database

Effective Temperature CO_2 (°C)

$$Effective\ Temperature\ CO_2 = \frac{log10(Average\ (12\ Month\ \ Temperature\ Correction\ Coefficient\ CO_2\ ))}{0.05}$$

** 0.05 is the slope of the temperature vs CO_2 flux function in our database

k600

$$k600\ =\ 0.24\ *\ (\ 2.51\ +\ 1.48\ *\ Annual\ Wind\ Speed\ at\ 10m^2\ +\ 0.39\ *\ Annual\ Wind\ Speed\ at\ 10m^2\ *\ log\ (\ Reservoir\ Area)\ )$$

** Vachon and Prairie (2013)

kh

$$kh\ =\ exp\ (\ (-115.6477\ -\ 6.1698\ *\ (Effective\ Temperature\ CH_4\ +\ 273.15)\ /\ 100\ )\ +\ (155.5756/\ ((Effective\ Temperature\ CH_4\ +\ 273.15)\ /\ 100)\ )\ +\ (\ 65.2553\ *\ ln\ ((Effective\ Temperature\ CH_4\ +\ 273.15)\ /\ 100)\ ))\ *\ (\ 1000\ /\ 18.0153\ )$$

** Handbook of Physics and Chemistry (1994)

pCH_4

$$pCH_4\ =\ 10^{(\ (\ 1.46\ +\ 0.03\ *\ Effective\ Temperature\ CH_4)\ -\ 0.29\ *\ log\ (Reservoir\ Area)\ )}$$

** Rasilo et al (2015)

Surface Water CH_4 Concentration

$$Surface\ Water\ CH_4\ Concentration\ =\ kh\ *\ pCH_4$$

CH_4 Emission Factor for Water Bodies (kg CH4/ha/yr)

$$CH_4\ Emission\ Factor\ for\ Water\ Bodies = Surface\ Water\ CH_4\ Concentration\ *\ k600\ *\ 16\ *\ \frac{365}{100}$$

q-bathymetric Shape

$$q - bathymetric\ shape\ = \frac{Maximum\ Depth}{Mean\ Depth}\ -\ 1$$

% Littoral Area

$$\%\ Littoral\ Area\ = \left(1 - \left(1 - \frac{3}{Maximum\ Depth}\right)^{q\_bathymetric\ shape}\right) * 100$$

Phosphorus Load Factor - Forest (kg/ha/yr)

$$Phosphorus\ Load\ factor\ -\ Forest = \frac{10^{(0.914 - log10\left(\left(\frac{Catchment\ Land\ Cover\ \% - Forest}{100}\right) * Catchment\ Area\right) * 0.014}}{100}$$

Phosphorus Load Factor- Croplands (kg/ha/yr)

$$Phosphorus\ Load\ factor\ -\ Croplands = \frac{10^{(1.818 - log10\left(\left(\frac{Catchment\ Land\ Cover\ \% - Croplands}{100}\right) * Catchment\ Area\right) * 0.227}}{100}$$

P Input from catchment (kgP yr-1)

$$P\ Input\ from\ catchment = \begin{pmatrix} Phosphorus\ Load\ factor - Croplands\ *\ Catchment\ Land\ Cover\ \% - Croplands \\ +Phosphorus\ Load\ factor - Forest\ *\ Catchment\ Land\ Cover\ \% - Forest \\ +Phosphorus\ Load\ factor - Wetlands\ *\ Catchment\ Land\ Cover\ \% - Wetlands \\ +Phosphorus\ Load\ factor - Settlements\ *\ Catchment\ Land\ Cover\ \% - Setttlements \\ +Phosphorus\ Load\ factor - Grassland/Shrubland\ *\ Catchment\ Land\ Cover\ \% - Grassland/Shrubland \\ +Phosphorus\ Load\ factor - Bare\ Areas\ *\ Catchment\ Land\ Cover\ \% - Bare\ Areas \\ +Phosphorus\ Load\ factor - Water\ Bodies\ *\ Catchment\ Land\ Cover\ \% - Water\ Bodies \\ +Phosphorus\ Load\ factor - Permanent\ Snow/Ice\ *\ Catchment\ Land\ Cover\ \% - Permanent\ Snow/Ice \end{pmatrix} * Catchment\ Area$$

**See table 12 for Load factor

P Human Input (kgP yr-1)

$$P\ Human\ input = Population\ in\ the\ catchment\ *\ 0{,}002\ *\ 365\ *\ \%\ Removal\ Wastewater\ \ Treatment$$

Population in the Catchment (person)

$$Population\ in\ the\ Catchment\ =\ Catchment\ Area\ *\ Population\ Density$$

Annual discharge (mm/yr)

$$Annual\ Discharge\ =\ Annual\ Runoff\ *\ 0.001\ *\ Catchment\ Area\ *\ 1000000/31536000$$

Water Residence Time (WRT, yrs)

$$WRT\ =\ \frac{Mean\ Depth\ *\ Reservoir\ Area}{Catchment\ Area\ *\ Annual\ Runoff} * 1000$$

River Area Before Impoundment (km²)

$$River\ Area\ Before\ Impoundment\ =\ \frac{River\ Length\ Before\ Impoundment * 5.9 * Catchment\ area^{0.32}}{1000000}$$

Reservoir Cumulative Global Horizontal Radiance (kWh /m²/period)

- If 40 > Latitude > -40:

$$Reservoir\ Cumulative\ Global\ Horizontal\ Radiance = (Average\ (12\ Month\ Reservoir\ Mean\ Global\ Horizontal\ Radiance) * Number\ of\ month\ over\ 0^\circ C * 30{,}4)$$

- If 40 < Latitude

$$Reservoir\ Cumulative\ Global\ Horizontal\ Radiance = (Average\ (May;\ June;\ July;\ August;\ September\ Reservoir\ Mean\ Global\ Horizontal\ Radiance) * Number\ of\ month\ over\ 0^\circ C * 30.4)$$

- If -40 > Latitude

$$Reservoir\ Cumulative\ Global\ Horizontal\ Radiance = (Average\ (November;\ December;\ January;\ February;\ March\ Reservoir\ Mean\ Global\ Horizontal\ Radiance) * Number\ of\ month\ over\ 0^\circ C * 30.4)$$

Conversion from Moles to Grams

In chemistry, a mole is Avogadro's number (6.02×10^{23}) of molecules (or anything) of a substance - so depending on the density of the substance, the mass of that amount of the substance could vary widely.

To convert from moles to grams one must first find the molar mass of the element or compound. Use the periodic table to read off the atomic mass from an element. If it is a compound, one must know the molecular formula; the total molar mass of the compound is deduced by adding up the atomic masses of each atom in the compound. The unit of the molar mass will be in grams per moles (g/mole).

Once you have the molar mass, you can easily convert from grams to moles, and from moles to grams.

- Number of moles = (# of grams) ÷ (molar mass)
- Number of grams = (# of moles) × (molar mass)

Table 8: Carbon dioxide and methane atomic (a) and molar (b) mass for most common GHG species in reservoirs

(a)

Element	Atomic mass (g/mol)
C	12
O	16
H	1

(b)

GHG	Molar mass (g/mol)
CO_2	44
CH_4	16

CO_2 Equivalents (CO_2e)

The international practice is to express GHG in CO_2 equivalents (CO_2e). Emissions of gases other than CO2 are translated into CO_2e by multiplying by the respective global warming potential (GWP).

Table 9: GWP relative to CO_2 at different time horizon for carbon dioxide and methane (IPCC 2013)

Gas name	Chemical formula	Global warming potential (GWP) for given time horizon	
		20-yr	100-yr
Carbon dioxide	CO_2	1	1
Methane	CH_4	86	34

Source: The IPCC considers the GWP of GHGs in a 100-year time frame.

It is important to note that care must be taken on the use of GWP as the conversion factor for calculation of gases' warming potential equivalences, as the IPCC GWP is not widely accepted to correctly represent the relative weight of the gases on the change in global temperature.

Conversion from "g of GHG" to "g of Carbon"

The conversion between "g of GHG" and "g of Carbon" is directly related to the ratio of the atomic mass of a GHG molecule to the atomic mass of a carbon atom. Essentially, this practice accounts for the carbon in the GHG molecule, as opposed to counting the entire molecule.

For carbon dioxide, the ratio of the atomic mass of a CO_2 molecule to the mass of a carbon atom is 44:12.

- To convert from "g of C" to "g of CO_2", multiply by 44/12
- To convert from "g of CO_2" to "g of C", multiply by 12/44
- Sometimes you find this noted as gC-CO_2 or tC-CO_2 (to make clear that these "g of C" refers to Carbon in a CO_2 molecule).

For methane, the ratio of the atomic mass of a CH_4 molecule to the mass of a carbon atom is 16:12.

- To convert from "g of C" to "g of CH_4", multiply by 16/12
- To convert from "g of CH_4" to "g of C", multiply by 12/16

It is important to make clear that these "g of C" refer to Carbon in a CH_4 molecule (i.e., not CO_2e – not considering GWP). It is common to use gC-CH_4 or tC-CH_4

Conversion from "g of Carbon" to "g of CO_2e"

With the use of CO_2 equivalents (CO_2e) it is possible to express emissions/removals of different GHG species on the same units of mass (g of CO_2e), allowing then to compare and to combine (add or subtract) these emissions.

To convert from "g of Carbon" to "g of CO_2e" it is necessary to:

- First convert from "g of C" to "g of GHG" (see item 3),
- And then multiply by the respective global warming potential (GWP) to obtain the "g of CO_2e".

For CO_2, as the GWP is 1, it is only necessary to convert from "g of C" to "g of CO_2", multiplying by 44/12.

For methane:

- First convert from "g of C-CH_4" to "g of CH_4", multiplying by 16/12
- And then, adopting the IPCC GWP for a 100-yr time-horizon, multiply by 34 to obtain the "g of CO_2e".

After converting the unit "g of Carbon" from the different GHG species in analysis to the unit "g of CO_2e", it is possible to compare the emissions or to add/subtract all values and then to obtain a total estimated emission expressed as "g of CO_2e".

It is also possible to express these values as "g of C-CO_2e" (grams of Carbon in the CO_2e), by multiplying the "g of CO_2e" by 12/44.

Carbon Dioxide Equivalents vs. Carbon Equivalents

While the international standard is to express emissions in CO_2 equivalents (CO_2e), many U.S.A. sources have expressed emissions data in terms of carbon equivalents (CE) in the past. In particular, the United States Environmental Protection Agency (USEPA) has used the carbon equivalent metric in the past for budget documents.

For the purposes of national greenhouse gas inventories, emissions are expressed as teragrams of CO_2 equivalent (Tg CO_2e). One teragram is equal to 10^{12} grams, or one million metric tons.

- To convert from CE to CO_2e, multiply by 44/12
- To convert from CO_2e to CE, multiply by 12/44

Annex IV - **Earth Engine**

To provide useful estimates of net GHG emissions from reservoirs, the G-res tool requires a lot of information concerning the physical, geographical, climatic, soil and land cover attributes of the reservoir itself as well as its catchment. However, this information needs to be extracted from the good and consistent sources. This process can be arduous and prone to error or inconsistencies. To facilitate this process, the G-res tool provides an additional functionality to help the user extract the information in a globally consistent manner to then enter the missing information manually within the G-res tool. This functionality was developed using Earth Engine platform of Google and it thus termed the Earth Engine (EE) functionality in the G-res tool. The information thus obtained can then be saved locally for future use.

The reservoir specific information that can be derived directly from the EE functionality are:

For the catchment:

- Catchment Area (in square kilometres)
- Catchment Annual Runoff (in millimeters per year)
- Population in the Catchment (person)
- Land Cover by Soil Type (in percentage)

For the reservoir:

- Dam Coordinates (in degrees, WGS84)
- Reservoir Area (in square kilometres)
- River length before impoundment (in meters)
- Maximum Depth (in meters)
- Mean Depth (in meters)
- Climate Zone
- Monthly Mean Temperature (in degree Celsius)
- Reservoir Mean Global Horizontal Radiance Annual (GHR) (in kilowatt hour per square meter per day)
- Reservoir Mean global horizontal Radiance (GHR) for the months of May to September (in kilowatt hour per square meter per day)
- Reservoir Mean Global Horizontal Radiance (GHR) for the months of November to March (in kilowatt hour per square meter per day)
- Soil Carbon Content in the Impounded Area (kilogram of carbon per square meters)
- Annual Wind Speed (meters per second)
- Land Cover by Soil Type (in percentage)

For the buffer surrounding the reservoir:

- Soil Carbon Content Buffer (kilogram of carbon per square meters)
- Land Cover by Soil Type (in percentage)

See complete User guide for step-by-step instructions available for download online in the G-res tool (www.hydropower.org/gres-tool) and on the G-res Tool website (g-res.hydropower.org) to accompany and facilitate the technical usage of the online Earth Engine tool.

WARNINGS concerning data output:

Catchment Annual Runoff vs Annual Discharge from the reservoir

The catchment annual runoff (in mm/year) is given by Earth Engine and asked in the G-res tool. Although, if the Annual Discharge (m^3/s) is available, please provide this value.

Reservoir Mean Global Horizontal Radiance (GHR)

Please choose one of the options:

- If 40 > Latitude > -40:

  Mean GHR Annual (kWh/m2/day)

- If Latitude > 40

  Mean GHR May to September (kWh/m2/day)

- If Latitude < -40

  Mean GHR November to March (kWh/m2/day)

River Area Before Impoundment vs Reservoir Water Bodies from Land Coverage categories

If the natural water body present before the impoundment of the reservoir is a **river**, please provide the River Length before Impoundment. As you are adding new information, your total percent might become higher than 100%. Please check what land coverage is in the immediate area of your river and modify those percent land coverage to obtain a total of maximum 100% (or a No data greater or equal to 0).

If the natural water body present before the impoundment of the reservoir is a **lake**, please use Earth Engine Water Bodies from the land coverage of the reservoir area before impoundment percent.

Annex V - Land Cover Categories Used in the Model Compared to the Categories from the European Space Agency (ESA) – Climate Change Initiative (CCI)

European Space Agency (ESA) – Climate Change Initiative (CCI) categories	IHA categories
No data	No Data
Cropland, rainfed	Croplands
Cropland, irrigated or post-flooding	
Tree or shrub cover	Forest
Tree cover, broadleaved, evergreen, closed to open (>15%)	
Tree cover, broadleaved, deciduous, closed to open (>15%)	
Tree cover, broadleaved, deciduous, closed (>40%)	
Tree cover, broadleaved, deciduous, open (15-40%)	
Tree cover, needleleaved, evergreen, closed to open (>15%)	
Tree cover, needleleaved, evergreen, closed (>40%)	
Tree cover, needleleaved, evergreen, open (15-40%)	
Tree cover, needleleaved, deciduous, closed to open (>15%)	
Tree cover, needleleaved, deciduous, closed (>40%)	
Tree cover, needleleaved, deciduous, open (15-40%)	
Tree cover, mixed leaf type (broadleaved and needleleaved)	
Mosaic tree and shrub (>50%) / herbaceous cover (<50%)	Grassland/Shrubland
Mosaic herbaceous cover (>50%) / tree and shrub (<50%)	
Shrubland	
Shrubland evergreen	
Shrubland deciduous	
Grassland	
Lichens and mosses	
Sparse vegetation (tree, shrub, herbaceous cover) (<15%)	
Sparse shrub (<15%)	
Sparse herbaceous cover (<15%)	
Mosaic cropland (>50%) / natural vegetation (tree, shrub, herbaceous cover)	
Mosaic natural vegetation (tree, shrub, herbaceous cover) (>50%) / cropland	
Herbaceous cover	
Tree cover, flooded, fresh or brakish water	Wetlands
Tree cover, flooded, saline water	
Shrub or herbaceous cover, flooded, fresh/saline/brakish water	
Urban areas	Settlements
Bare areas	Bare Areas
Consolidated bare areas	
Unconsolidated bare areas	
Water bodies	Water Bodies
Permanent snow and ice	Permanent

Annex VI - Emission Factors and Export Coefficient

Emission Factors of Land Cover on Upland Mineral Soils

Upland mineral land cover types include those land cover types and land use types that reside on non-waterlogged, mineral soils. The catchment area landscape may consist of unmanaged land, e.g., forests, grasslands, bare soils etc. and managed land types such as croplands, managed forests, settlements, roads etc. Table 10 shows the default C balance figures used as emission factors for upland forests. While forests are considered net C sinks by default, all the other upland mineral soil land cover types, following the 2006 IPCC AFOLU Guidelines (IPCC 2006) are considered as carbon neutral (their EF = 0). If the local conditions are strikingly different from those assumptions, the User is envisaged to change the emission factors according to better knowledge. When the G-res tool outcomes are reported, the User should transparently describe all possible changes in emission factors, applied in the net GHG balance calculations of the User specified systems.

Table 10: The stock change values (1990-1999) in t C /ha/yr, as pooled by biomes (Pan et al. 2011). Negative signs indicate that forests in all biomes serve as net C sinks

Biome	Stock change value (tC/ha/yr)
Boreal	-0.4
Temperate	-0.9
Tropical intact	-0.8
Tropical regrowth	-3.2
All tropics (Tropical and Sub-Tropical)	-1.4
Global total	-1.0

Emission Factors of Land Cover on Organic Soils

Default emission factors concerning the land cover/land use types on organic soils are simplified from a more comprehensive breakdown. If the User needs to update or improve the accuracy of emission factors from organic soils, introduction of known carbon losses from the organic land use areas can be helpful (see Table 10).

Waterlogged soils behave differently from dry upland soils in that the organic matter may accumulate in greater quantities due to absence of oxygen and low rate of decay in anoxic conditions. Natural wetlands are typically sinks of organic carbon and show net removals of CO_2. At the same time, anoxic soil or sediment gives raise to CH_4. In such more complex cases, net fluxes of both gases need to be considered in order to assess the complete impact of net GHG emissions or removals. Comparison of the GHG impact of different gases is based on a model that converts the warming impact of other gases to correspond to that of CO_2 integrated over certain time span of residence of the gas in the atmosphere (IPCC 2006).

The impact of a CO_2 molecule is considered equal to 1. As CO_2 equivalent, the warming impact of a CH_4 molecule is 34 and that of N_2O is 298 (IPCC Assessment Report 5, 2013).

Land use change can dramatically alter the landscape's GHG balance. After drainage of peatlands by ditching for forestry or agriculture, the earlier net removals balance of peatlands may turn to strong net emissions due to heavily increased oxic decay of organic matter. At the same time, anaerobic decomposition and methanogenesis is inhibited by establishment of oxic conditions. Large net C losses can sometimes be expected even while growth of trees and other upland vegetation improves. Because of the different nature of GHG exchange in upland mineral soil ecosystems from that of waterlogged ecosystems, the G-res tool provides default emission factors separately for mineral soil and organic soil ecosystems. Land use for same purposes can take place either in upland mineral soils and organic soils.

Table 11: CH_4 (kg CH_4/ha/yr) and CO_2 (t CO_2-C/ha/yr) emission factor for the land cover categories in mineral and organic soil for the four (4) type of climate (Boreal, Temperature, Sub-tropical and Tropical)

Climate	Emissions factor type	Soil type	Cropland	Bare Areas	Wetlands	Forest	Grassland/ Shrubland	Urban Areas	Water Bodies
Boreal	CH_4 Emission Factor (kg CH_4/ha/yr)	Mineral Soil	0	0	0	0	0	0	Calculated following Rasilo et al 2015 and Vachon and Prairie 2013
		Organic Soil	0	6.1	89	4.5	1.4	19.6	
	CO_2 Emission Factor (t CO_2-C/ha/yr)	Mineral Soil	0	0	0	-0.4	0	0	n/a
		Organic Soil	7.9	2.8	-0.5	0.6	5.7	6.4	
Temperate	CH_4 Emission Factor (kg CH_4/ha/yr)	Mineral Soil	0	0	0	0	0	0	Calculated following Rasilo et al 2015 and Vachon and Prairie 2013
		Organic Soil	0	6.1	0	0	18.9	19.6	
	CO_2 Emission Factor (t CO_2-C/ha/yr)	Mineral Soil	0	0	0	-0.9	0	0	n/a
		Organic Soil	7.9	2.8	-0.5	0	5	6.4	

Sub-tropical	CH_4 Emission Factor (kg CH_4/ha/yr)	Mineral Soil	0	0	0	0	0	0	Calculated following Rasilo et al 2015 and Vachon and Prairie 2013
		Organic Soil	0	7	116.3	2.5	7	19.6	
	CO_2 Emission Factor (t CO_2-C/ha/yr)	Mineral Soil	0	0	0	-1.4	0	0	n/a
		Organic Soil	11.7	2	0.1	2.6	9.6	6.4	
Tropical	CH_4 Emission Factor (kg CH_4/ha/yr)	Mineral Soil	0	0	0	0	0	0	Calculated following Rasilo et al 2015 and Vachon and Prairie 2013
		Organic Soil	75	7	41	1.8	7	19.6	
	CO_2 Emission Factor (t CO_2-C/ha/yr)	Mineral Soil	0	0	0	-1.4	0	0	n/a
		Organic Soil	11.7	2	0	15.3	9.6	6.4	

Table 12: Phosphorus load factor for the land cover categories at low and high land use intensity (kg/ha/yr)

Land cover	Low land use intensity P load (kg/ha/yr)	High land use intensity P load (kg/ha/yr)
Bare Areas	0.31	
Croplands	$10^{(1.818 - 0.227*\log10(\text{Cropland area in the catchment}))}$ *	2.24
Forest	$10^{(0.914 - 0.014*\log10(\text{Forest area in the catchment}))}$ *	0.41
Grassland/Shrubland	0.26	42.86
Permanent Snow/Ice	0.15	
Settlements	2.75	
Water bodies	0	
Wetlands	0.1	

* Prairie and Kalff (1986)

Annex VII – **Literature Review References**

Åberg, J., Bergström, A. K., Algesten, G., Söderback, K., & Jansson, M. (2004). A comparison of the carbon balances of a natural lake (L. Örträsket) and a hydroelectric reservoir (L. Skinnmuddselet) in northern Sweden. *Water Research*, *38*, 531–538. doi:10.1016/j.watres.2003.10.035

Abril, G., Guérin, F., Richard, S., Delmas, R., Galy-Lacaux, C., Gosse, P., & Matvienko, B. (2005). Carbon dioxide and methane emissions and the carbon budget of a 10-year old tropical reservoir (Petit Saut, French Guiana). *Global Biogeochemical Cycles*, *19*(GB4007), 1–16. doi:10.1029/2005GB002457

Arntzen, E., Miller, B., & O'Toole, A. (2013). Evaluating greenhouse gas emissions from hydropower complexes on large rivers in Eastern Washington, (March).

Barros, N., Cole, J. J., Tranvik, L. J., Prairie, Y. T., Bastviken, D., Huszar, V. L. M., Roland, F. (2011a). Carbon emission from hydroelectric reservoirs linked to reservoir age and latitude. *Nature Geoscience*, *4*(7), 593–596. doi:10.1038/ngeo1211

Barros, N., Cole, J. J., Tranvik, L. J., Prairie, Y. T., Bastviken, D., Huszar, V. L. M., & Roland, F. (2011b). Supplementary information: Carbon emission from hydroelectric reservoirs linked to reservoir age and latitude. *Nature Geoscience*, *4*, 593–596. doi:10.1038/ngeo1211

Bastien, J., & Demarty, M. (2013). Spatio-temporal variation of gross CO2 and CH4 diffusive emissions from Australian reservoirs and natural aquatic ecosystems, and estimation of net reservoir emissions. *Lakes and Reservoirs: Research and Management*, *18*, 115–127. doi:10.1111/lre.12028

Bastien, J., Tremblay, A., & LeDrew, L. (2009). Greenhouse gases fluxes from smallwood reservoir and natural water bodies in Labrador, Newfoundland, Canada. *Verh. Int. Ver. Limnol.*, *30*(6), 858–861.

Bergier, I., Novo, E. M. L. M., Ramos, F. M., Mazzi, E. a., & Rasera, M. F. F. L. (2011). Carbon Dioxide and Methane Fluxes in the Littoral Zone of a Tropical Savanna Reservoir (Corumbá, Brazil). *Oecologia Australis*, *15*(3), 666–681. doi:10.4257/oeco.2011.1503.17

Bergström, A.-K., Algesten, G., Sobek, S., Tranvik, L., & Jansson, M. (2004). Emission of CO2 from hydroelectric reservoirs in northern Sweden. *Archiv für Hydrobiologie*, *159*(January), 25–42. doi:10.1127/0003-9136/2004/0159-0025

Cailleaud, E., Serça, D., & Guérin, F. (2015). *Doctorat de l'université de toulouse*. *Thesis, Université de Toulouse*.

Chanudet, V., Descloux, S., Harby, A., Sundt, H., Hansen, B. H., Brakstad, O., & Guerin, F. (2011). Gross CO2 and CH4 emissions from the Nam Ngum and Nam Leuk sub-tropical reservoirs in Lao PDR. *Science of the Total Environment*, *409*(24), 5382–5391. doi:10.1016/j.scitotenv.2011.09.018

Chen, H., Yuan, X., Chen, Z., Wu, Y., Liu, X., Zhu, D., … Li, W. (2011). Methane emissions from the surface of the Three Gorges Reservoir. *Journal of Geophysical Research: Atmospheres*, *116*(D21306), 1–5. doi:10.1029/2011JD016244

Delmas, R., & Galy-lacaux, C. (2001). Emissions of greenhouse gases from the tropical

hydroelectric reservoir of Petit Saut (French Guiana) compared with emissions would be similar to emissions from a gas power plant producing the including aboveglround vegetation t (C) ha -1) and, *15*(4), 993–1003.

DelSontro, T., Mcginnis, D. F., Sobek, S., Ostrovsky, I., & Wehrli, B. (2010). Extreme methane emissions from a swiss hydropower Reservoir: Contribution from bubbling sediments. *Environmental Science and Technology*, *44*(7), 2419–2425. doi:10.1021/es9031369

DelSontro T, Kunz MJ, Kempter T, Wüest A, Wehrli B, Senn DB. (2011). Spatial heterogeneity of methane ebullition in a large tropical reservoir. *Environmental Science and Technology* 45: 9866–9873.

Demarty, M., & Bastien, J. (2011). *GHG emissions from hydroelectric reservoirs in the tropical and equatorial regions: Focus on CH 4 emissions*. Montréal.

Demarty, M., Bastien, J., Tremblay, A., Hesslein, R. H., & Gill, R. (2009). Greenhouse gas emissions from boreal reservoirs in Manitoba and Québec, Canada, measured with automated systems. *Environmental Science and Technology*, *43*(23), 8908–8915. doi:10.1021/es8035658

Deshmukh, C. (2013). *Greenhouse gas emissions (CH4, CO2 and N2O) from a newly flooded hydroelectric reservoir in subtropical South Asia : The case of Nam Theun 2 Reservoir, Lao PDR*.

Deshmukh, C., & Serça, D. (2014). Physical controls on CH4 emissions from a newly flooded subtropical freshwater hydroelectric reservoir: Nam Theun 2. *Biogeosciences*, 4251–4269. doi:10.5194/bg-11-4251-2014

Diem, T. (2008). *Methane dynamics in oxic and anoxic aquatic systems*.

Duchemin, É. (2000). *Hydroélectricité et gaz à effet de serre évaluation des émissions des différents gaz et identification des processus biogéochimiques de leur production*.

Duchemin, E., Lucotte, M., Canuel, R., & Chamberland, a. (1995). Production of the greenhouse gases CH4 and CO2 by hydroelectric reservoirs of the boreal region. *Global Biogeochemical Cycles*, *9*(4), 529–540. doi:10.1029/95GB02202

Fearnside, P. M. (1997). Greenhouse-gas emissions from Amazonian hydroelectric reservoirs: the example of Brazil's Tucuruí Dam as compared to fossil fuel alternatives. *Environmental Conservation*, *24*(1), 64–75. doi:10.1017/S0376892997000118

Fearnside, P. M. (2000). Greenhouse gas emissions from a hydroelectric reservoir (Brazil's Tucuruí dam) and the energy policy implications. *Phd proposal*. *National Institute for Research in the Amazon (INPA).*

Fearnside, P. M. (2008). A Framework for Estimating Greenhouse Gas Emissions from Brazil's Amazonian Hydroelectric Dams. *Oecologia Brasiliensis*, *12*(01), 100–115. doi:10.4257/oeco.2008.1201.11

Galy-Lacaux, C., Delmas, R., Jambert, C., Dumestre, J.-F., Labroue, L., Richard, S., & Gosse, P. (1997). Gaseous emissions and oxygen consumption in hydroelectric dams: A case study in French Guyana. *Global Biogeochemical Cycles*, *11*(4), 471–483. doi:10.1029/97GB01625

Galy-Lacaux, C., Delmas, R., Kouadio, G., Richard, S., & Gosse, P. (1999). Long-term greenhouse gas emissions from hydroelectric reservoirs in tropical forest regions • Georges Kouadio ,: Sandfine and Philippe Gosse maximum Then the time course of dissolved over the three average dissolved methane concentrations were lower and r.

Global Biogeochemical Cycles, *13*(2), 503–517.

Grinham, A., Dunbabin, M., Gale, D., & Udy, J. (2011). Quantification of ebullitive and diffusive methane release to atmosphere from a water storage. *Atmospheric Environment*, *45*(39), 7166–7173. doi:10.1016/j.atmosenv.2011.09.011

Gruca-Rokosz, R., Tomaszek, J. a., Koszelnik, P., & Czerwieniec, E. (2011). Methane and carbon dioxide emission from some reservoirs in SE Poland. *Limnological Review*, *10*(1), 15–21. doi:10.2478/v10194-011-0002-8

Guérin, F., Abril, G., Richard, S., Burban, B., Reynouard, C., Seyler, P., & Delmas, R. (2006). Methane and carbon dioxide emissions from tropical reservoirs: Significance of downstream rivers. *Geophysical Research Letters*, *33*(L21407), 1–6. doi:10.1029/2006GL027929

Hall, M., West, J., Lane, J., de Haas, D., & Sherman, B. (2009). *Energy and greenhouse gas emissions for SEQ Water Strategy*. *Urban Water Security Reasearch Alliance*.

Hällqvist, E. (2012). *Methane emissions from three tropical hydroelectrical reservoirs*. Uppsala Universitet.

Harby, A., Guerin, F., Bastien, J., & Demarty, M. (2012). *Greenhouse gas status of hydro reservoirs*.

Huttunen, J. T., Väaisäanen, T. S., Hellsten, S. K., Heikkinen, M., Nykänen, H., Jungner, H., & Martikainen, P. J. (2002). O in hydroelectric reservoirs Lokka and Porttipahta in the northern boreal zone in Finland. *Global Biogeochemical Cycles*, *16*(1), 1–17. doi:10.1029/2000GB001316

Keller, M., & Stallard, R. F. (1994). Methane emission by bubbling from Gatun Lake, Panama. *Journal of Geophysical Research*, *99*(92), 8307–8319. doi:10.1029/92JD02170

Kelly, C. a., Rudd, J. W. M., St. Louis, V. L., & Moore, T. (1994). Turning attention to reservoir surfaces, a neglected area in greenhouse studies. *Eos, Transactions American Geophysical Union*, *75*(29), 332–333. doi:10.1029/94EO00987

Kemenes, A., Forsberg, B. R., & Melack, J. M. (2007). Methane release below a tropical hydroelectric dam. *Geophysical Research Letters*, *34*(L12809), 1–5. doi:10.1029/2007GL029479

Maeck, A., DelSontro, T., McGinnis, D. F., Fischer, H., Flury, S., Schmidt, M., & Lorke, A. (2013). Sediment Trapping by Dams Creates Methane Emission Hot Spots. *Environ. Sci. Technol*, *47*, 8130–3137. doi:10.1021/es4003907

Matvienko, B. (n.d.). *Methane release – predictive models for hydroelectric reservoirs*.

Musenze, R. S., Grinham, A., Werner, U., Gale, D., Sturm, K., Udy, J., & Yuan, Z. (2014). Assessing the Spatial and Temporal Variability of Di ff usive Methane and Nitrous Oxide Emissions from Subtropical Freshwater Reservoirs. *Environmental Science & Technology*, *48*, 14499–14507.

Nirmal Rajkumar, A., Barnes, J., Ramesh, R., Purvaja, R., & Upstill-Goddard, R. C. (2008). Methane and nitrous oxide fluxes in the polluted Adyar River and estuary, SE India. *Marine Pollution Bulletin*, *56*(12), 2043–2051. doi:10.1016/j.marpolbul.2008.08.005

Ometto, J. P., Cimbleris, A. C. P., Dos Santos, M. a., Rosa, L. P., Abe, D., Tundisi, J. G., & Roland, F. (2013). Carbon emission as a function of energy generation in hydroelectric reservoirs in Brazilian dry tropical biome. *Energy Policy*, *58*, 109–116. doi:10.1016/j.enpol.2013.02.041

Pacheco, F. S., Soares, M. C. S., Assireu, a. T., Curtarelli, M. P., Abril, G., Stech, J. L., & Ometto, J. P. (2015). The effects of river inflow and retention time on the spatial heterogeneity of chlorophyll and water–air CO_2 fluxes in a tropical hydropower reservoir. *Biogeosciences*, *12*, 147–162. doi:10.5194/bg-12-147-2015

Panneer Selvam, B., Natchimuthu, S., Arunachalam, L., & Bastviken, D. (2014). Methane and carbon dioxide emissions from inland waters in India - implications for large scale greenhouse gas balances. *Global Change Biology*, *20*(11), 3397–3407. doi:10.1111/gcb.12575

Panneer Selvam, B., Natchimuthu, S., & Bastviken, D. (2014). Methane and carbon dioxide emissions from inland waters in India - Supporting information. *Global Change Biology*, *20*(11), 8.

Roehm, C., & Tremblay, A. (2006). Role of turbines in the carbon dioxide emissions from two boreal reservoirs, Québec, Canada. *Journal of Geophysical Research Atmospheres*, *111*(24), 1–9. doi:10.1029/2006JD007292

Roland, F., Vidal, L. O., Pacheco, F. S., Barros, N. O., Assireu, A., Ometto, J. P. H. B., … Cole, J. J. (2010). Variability of carbon dioxide flux from tropical (Cerrado) hydroelectric reservoirs. *Aquatic Sciences*, *72*, 283–293. doi:10.1007/s00027-010-0140-0

Rosa, L. P., Aurelio, M., Santos, D. O. S., Matvienko, B., Oliveira, E., & Sikar, E. (2004). Greenhouse gas emissions from hydroelectric reservoirs in tropical regions. *Climatic Change*, *66*, 9–21.

Rosa, L., Santos, M. Dos, Matvienko, B., & Sikar, E. (2002). *Hydroelectric reservoirs and global warming*. *Proceedings of the Rio*.

Santos, M. A., Rosa, L. P., Sikar, B., Sikar, E., & dos Santos, E. O. (2006). Gross greenhouse gas fluxes from hydro-power reservoir compared to thermo-power plants. *Energy Policy*, *34*, 481–488. doi:10.1016/j.enpol.2004.06.015

Sherman, B., & Ford, P. (2011). Methane Emissions from Two Reservoirs in a Steep , Sub-Tropical Rainforest Catchment. *Science Forum and Stakeholder Engagement: Building Linkages, Collaboration and Science Quality*, 1–9.

Sherman, B., Ford, P., Mitchell, A., & Hancock, G. (2001). *Greenhouse gas emissions from reservoirs - is Australian hydropower environmentally friendly?*

Sikar, E., Dos Santos, M. A., Matvienko, B., Silva, M. B., Rocha, C. H. E. D., Santos, E., & Junior, A. P. B. (2005). Greenhouse gases and initial findings on the carbon circulation in two reservoirs and their watersheds. *Verh. Internat. Verein. Limnol.*, *29*(July), 1–4.

Sikar, E., Matvienko, B., Santos, M. A., Rosa, L. P., Silva, M. B., Santos, E. O., & Jr, A. P. S. (2009). Tropical reservoirs are bigger carbon sinks than soils. *Verh. Internat. Verein. Limnol.*, *30*(April), 838–840.

Smith, L. K., & Lewis, W. M. (1992). Seasonality of methane emissions from five lakes and associated wetlands of the Colorado Rockies. *Global Biogeochemical Cycles*. doi:10.1029/92GB02016

Soumis, N., Duchemin, É. , Canuel, R., & Lucotte, M. (2004). Greenhouse gas emissions from reservoirs of the western United States. *Global Biogeochemical Cycles*, *18*(GB3022), 1–11. doi:10.1029/2003GB002197

St. Louis, V. L., Kelly, C. a., Duchemin, É., Rudd, J. W. M., & Rosenberg, D. M. (2000). Reservoir surfaces as sources of greenhouse gases to the atmosphere: A global estimate.

BioScience, *50*(9), 766–775. doi:10.1641/0006-3568(2000)050[0766:RSASOG]2.0.CO;2

Sturm, K., Yuan, Z., Gibbes, B., Werner, U., & Grinham, A. (2014). Methane and nitrous oxide sources and emissions in a subtropical freshwater reservoir, South East Queensland, Australia. *Biogeosciences*, *11*(18), 5245–5258. doi:10.5194/bg-11-5245-2014

Tadonléké, R. D., Marty, J., & Planas, D. (2012). Assessing factors underlying variation of CO2 emissions in boreal lakes vs. reservoirs. *FEMS Microbiology Ecology*, *79*, 282–297. doi:10.1111/j.1574-6941.2011.01218.x

Tamooh F, Borges a. V., Meysman FJR, Van Den Meersche K, Dehairs F, Merckx R, & Bouillon S. (2013). Dynamics of dissolved inorganic carbon and aquatic metabolism in the Tana River basin, Kenya. *Biogeosciences* 10: 6911–6928.

Tavares Lima, I. B. (2005). Biogeochemical distinction of methane releases from two Amazon hydroreservoirs. *Chemosphere*, *59*, 1697–1702. doi:10.1016/j.chemosphere.2004.12.011

Tavares Lima, I. B., Novo, E. M. L. de M., Ballester, M. V. R., & Ometto, J. P. (1998). Methane Production, Transport and Emission in Amazon Hydroelectric Plants. In *Geoscience and Remote Sensing Symposium Proceedings* (Vol. 5, pp. 2529–2531).

Teodoru, C. R., Bastien, J., Bonneville, M. C., Del Giorgio, P. a., Demarty, M., Garneau, M., & Tremblay, A. (2012). The net carbon footprint of a newly created boreal hydroelectric reservoir. *Global Biogeochemical Cycles*, *26*(GB2016), 1–14. doi:10.1029/2011GB004187

Therrien, J., Tremblay, A., & Jacques, R. B. (2005). 9 CO2 Emissions from Semi-Arid Reservoirs and Natural Aquatic Ecosystems. In *Greenhouse Gas Emissions—Fluxes and Processes* (pp. 233–250).

Tremblay, A., Demers, C., & Bastien, J. (2009). *GHG Fluxes (CO2, CH4, N2O) Before and During the First Three Years After Impoundment At the Eastmain 1 Reservoir (Quebec, Canada)*.

Tremblay, A., Therrien, J., Hamlin, B., Wichmann, E., & Ledrew, L. J. (2005). Chap. 8 GHG Emissions from Boreal Reservoirs and Natural Aquatic Ecosystems. In *Greenhouse Gas Emissions—Fluxes and Processes* (pp. 209–232).

Tremblay, A., Varfalvy, L., & Lambert, M. (2008). Greenhouse gases from boreal hydroelectric reservoirs : 15 years of data ?

Trojanowska, A., Kurasiewicz, M., Plesniak, L., & Jedrysek, M. O. (2009). Emission of Methane From Sediments of Selected Polish Dam Reservoirs. *Teka Kom. Ochr. Kszt. Środ. Przyr.*, *6*, 368–373.

Wang, F., Cao, M., Wang, B., Fu, J., Luo, W., & Ma, J. (2015). Seasonal variation of CO2 diffusion flux from a large subtropical reservoir in East China. *Atmospheric Environment*, *103*, 129–137.

Wang, S., Jiao, L., Yang, S., Jin, X., Liang, H., & Wu, F. (2011). Organic matter compositions and DOM release from the sediments of the shallow lakes in the middle and lower reaches of Yangtze River region, China. *Applied Geochemistry*, *26*(8), 1458–1463. doi:10.1016/j.apgeochem.2011.05.019

Xiao, S., Liu, D., Wang, Y., Yang, Z., & Chen, W. (2013). Temporal variation of methane flux from Xiangxi Bay of the Three Gorges Reservoir. *Scientific reports*, *3*, 2500. doi:10.1038/srep02500

Yang L, Lu F, Zhou X, Wang X, Duan X, & Sun B. (2014). Progress in the studies on the greenhouse gas emissions from reservoirs. *Acta Ecologica Sinica* 34: 204–212.

Zhao, Y., Wu, B. F., & Zeng, Y. (2013). Spatial and temporal patterns of greenhouse gas emissions from Three Gorges Reservoir of China. *Biogeosciences*, *10*, 1219–1230. doi:10.5194/bg-10-1219-2013

Annex VIII - **GIS Work**

Reservoirs

For the most part, reservoir delineations were obtained directly from the GRaND database. Reservoirs missing from this database were delineated with the "Imagery" layer (Web Mercator Auxiliary Sphere projection [EPSG : 3857] in the WGS 84 datum) from the Basemaps of ArcGIS 10.1.

Values as reservoir elevation, temperature, and wind speed data were extracted with the "Zonal Stats" plugin in QGIS 2.8.1 (Wien).

Catchments

Catchment delineations were extracted from the Hydrobasins database (http://hydrosheds.org/page/hydrobasins , Lehner and Grill 2013). Catchments missing from this database were delineated with the "Hydrology" toolbox in the "Spatial Analyst" extension in ArcGIS 10.1.

Values as catchment average annual runoff, population density, precipitation, soil carbon content, net primary production (NPP), elevation, and mean slope data were extracted with the "Zonal Stats" plugin in QGIS 2.8.1 (Wien). The mean slopes were calculated with the "Slope" tool in the "Surface" toolbox in the "Spatial Analyst" extension in ArcGIS 10.1. The percentages of each land cover category in the watersheds were determined with the "Tabulate Intersection" tool in the "Statistics" toolbox in the "Analysis Tools" extension in ArcGIS 10.1.

Reservoirs and Catchment Area and Perimeter

Area and perimeter data, for both the reservoirs and the catchments, were calculated with ArcGIS 10.1 in the World Cylindrical Equal Area projection (EPSG: 3410) in the WGS 84 datum.

Reservoir Elevation, Catchment Delineation, Catchment Mean Elevation, Catchment Mean Slope and Catchment Delineation

For most of the reservoirs (between 60°N and 60°S), their elevation and the delineation of their catchment was determined with the digital elevation model (DEM) of the Shuttle Radar Topography Mission (SRTM).

For the rest of the reservoir, as well as the mean elevation and the mean slope of all the reservoirs, the data was derived from the GTOPO30 Digital Elevation Model (DEM).

Annex IX - Validation of the Buffer Method Used to Generate Pre-Impoundment Land Cover Data for Existing Reservoirs

Overview of the Buffer Method

Global mapping of land cover before 1993 is very limited and therefore it is not possible to specifically identify land cover at these locations. A method was developed to provide an estimate of the land cover by comparing the Pre-impoundment land cover with the land cover around the edge of the reservoir post-impoundment, both of which could be determined from global mapping. A relationship between these could then be determined and applied to reservoirs that have no global mapping source for the Pre-impoundment condition. This is called the 'Buffer method'.

Data from 278 reservoirs worldwide located from the Lehner et al (2011) database was used to evaluate the land cover from mapping data for reservoirs that were impounded after 1993. To demonstrate the validity of the buffer method, the land cover distribution of the reservoirs in both the areas delimited by the buffer and the real inundated area were analysed. The percentage of each land cover class extracted the buffer zone was compared to the percentage of each land cover class extracted from satellite images of the inundated area. All land cover data are extracted from AVHRR global land cover map.

The percentage of conserved land cover is the total share of LC which is identified with the same LC class in the buffer area and inundated area. Using the land cover categories, more than 68 % of the studied reservoirs have a percentage of conserved LC higher than 70 % (Figure 13), and 8 % have a percentage of conserved LC smaller than 50 %.

Using the GHG Screening Tool LC classification (Annex V), more than 84 % of the studied reservoirs have a percentage of conserved LC higher than 70 % (Figure 13), and 4 % have a percentage of conserved LC smaller than 50 %.

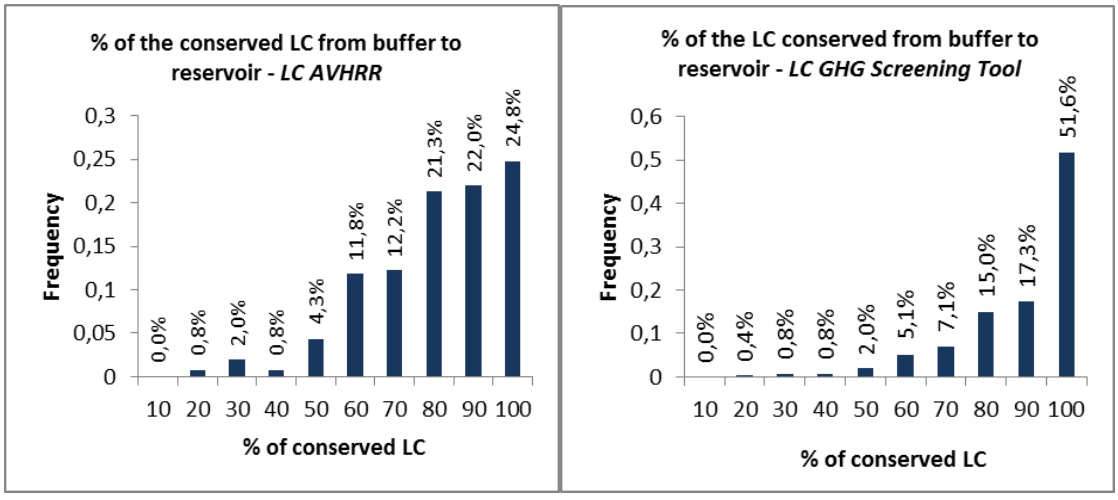

Figure 9: Percentage of Land Cover conserved from the buffer area to the reservoir area for the AVHRR land cover categories (left) and for the GHG Screening Tool LC classes (right)

Limitations of the Buffer Method

Reservoir Area – Buffer Size

Most of the reservoirs are relatively small: 166 reservoirs among the 278 studied reservoirs have an area less than 10 km² (Figure 10).

The percentage of conserved land cover as a function of reservoir area (Figure 15 upper) shows that the larger the reservoir area is, the higher the percentage of conserved land cover is. Some reservoirs with an area smaller than 5 km2 have less than 50 % conserved LC.

The percentage of conserved land cover as a function of buffer size (Figure 15 lower) shows the larger the buffer width is, the higher the percentage of conserved land cover is. Some reservoirs with buffer width smaller than 1 km have less than 50 % conserved land cover.

Given the definition of the buffer dimension, the smaller the reservoir area is, the smaller the buffer width will be and therefore the less the buffer method validity is predictable.

The limitation of the Buffer method is highly correlated to the pixel resolution of the satellite images used to extract the LC data. In our case, the AVHRR land cover categories resolution is 1 km x 1 km. As a consequence, the buffer method for reservoirs whose buffer has a width smaller than 1 km might give inaccurate results.

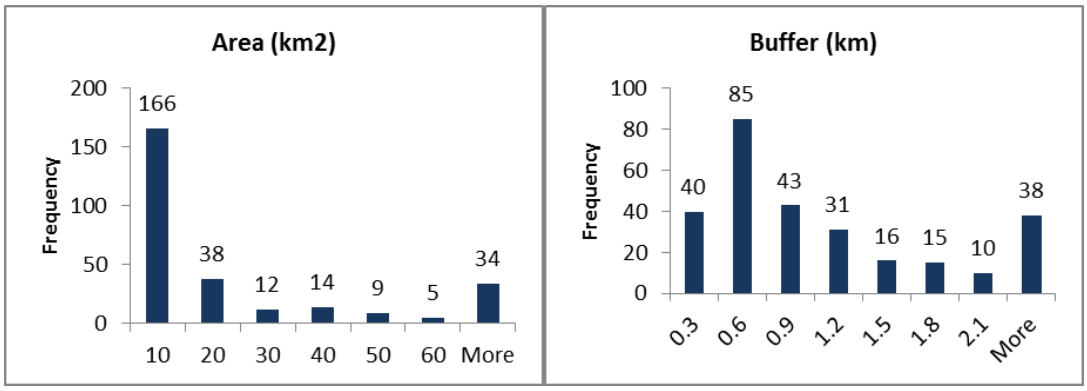

Figure 10: Histograms of area distribution (left) and buffer width zone distribution (right) for the 278 reservoirs impounded after 1993

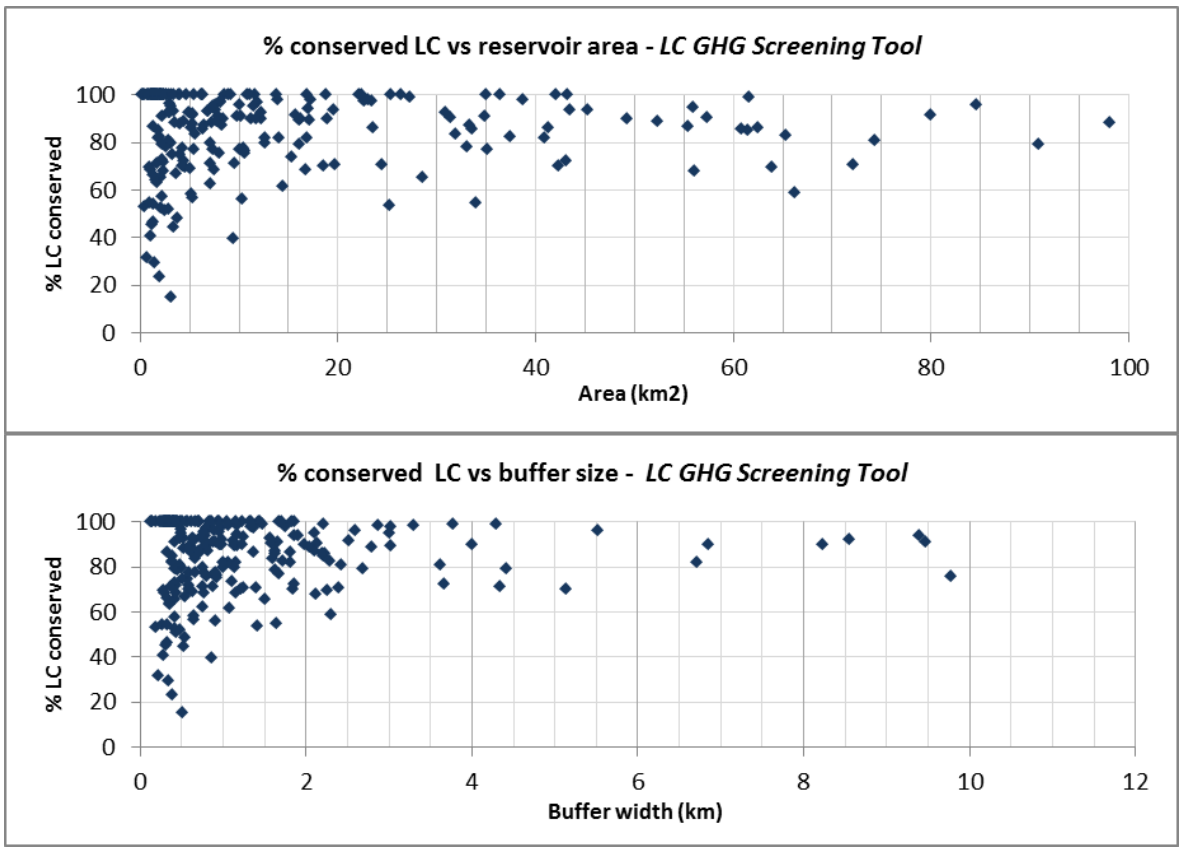

Figure 11: Percentage of conserved LC as a function of reservoir area (upper) and buffer size (lower)

Reservoir Elevation and Latitude

Figure 16 shows the histograms of elevation and latitude distributions: 199 reservoirs among the 278 studied ones are located at elevation levels lower than 600 m a.s.l. (Figure 16 left); 201 reservoirs among the 278 studied ones are located at latitudes in the range ± [20 - 50] degree (Figure 16 right).

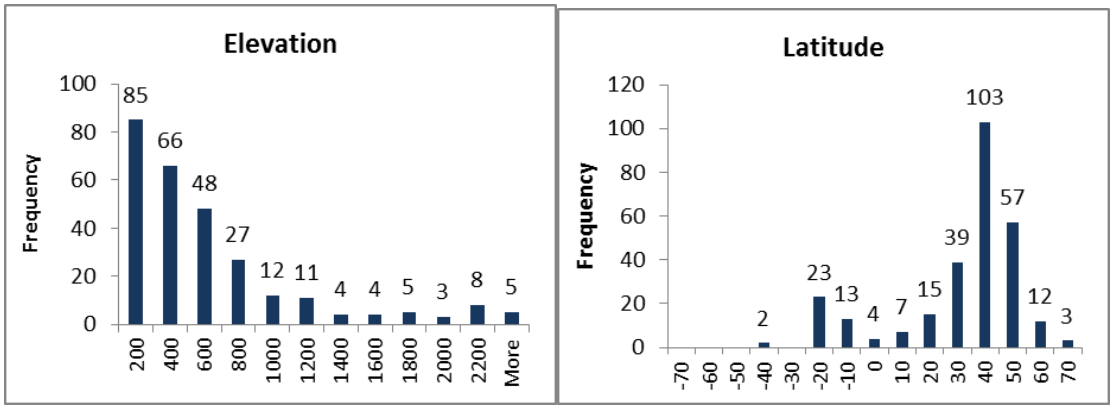

Figure 12: Histograms of elevation distribution (left) and latitude distribution (right) for the 278 reservoirs impounded after 1993

The percentage of conserved land cover as a function of reservoir altitude (Figure 16) shows the percentage of conserved land cover is over 70 % for reservoirs with elevation higher than 700 m while it is in the range of 15-100 % for reservoirs with elevation lower than 700 m.

The percentage of conserved land cover as a function of reservoir latitude (Figure 16) shows the percentage of conserved land cover is over 60 % for reservoirs with latitude in the range ± 0-20 and ± 50-70 degrees. The percentage of conserved land cover are lower for reservoirs with latitude in the range ± 20-50 degrees.

The buffer method gives better results for reservoirs at high altitudes and reservoirs at northern or equatorial latitudes. The main reasons are likely to be that:

- Mountain reservoirs, northern boreal reservoirs as well as equatorial reservoirs might be more isolated from population than reservoirs located at mid-latitudes with higher population density. For these cases the reservoir surroundings are probably more similar to the inundated area because of little human modifications of Land cover and Land use.

- There might be few data for reservoirs located at high altitudes to statistically demonstrate the method.

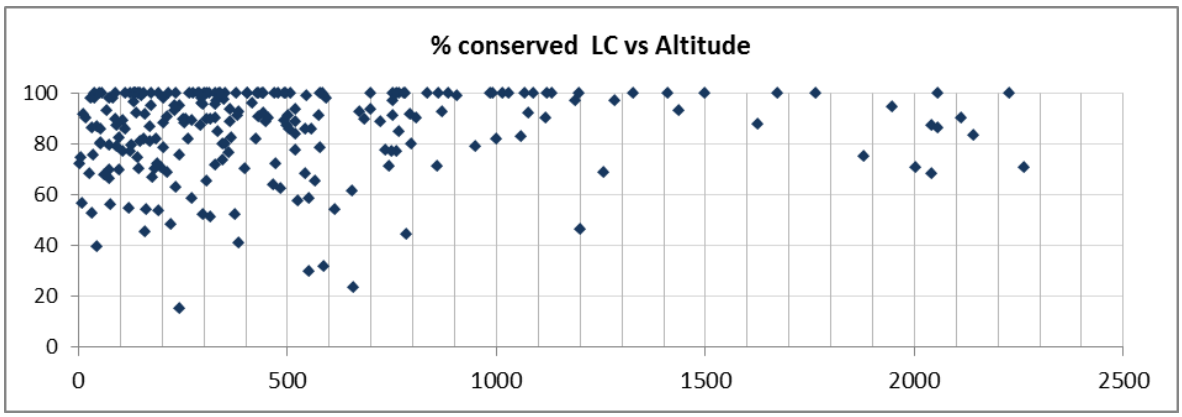

Figure 13: Percentage of conserved LC as a function of reservoir altitude

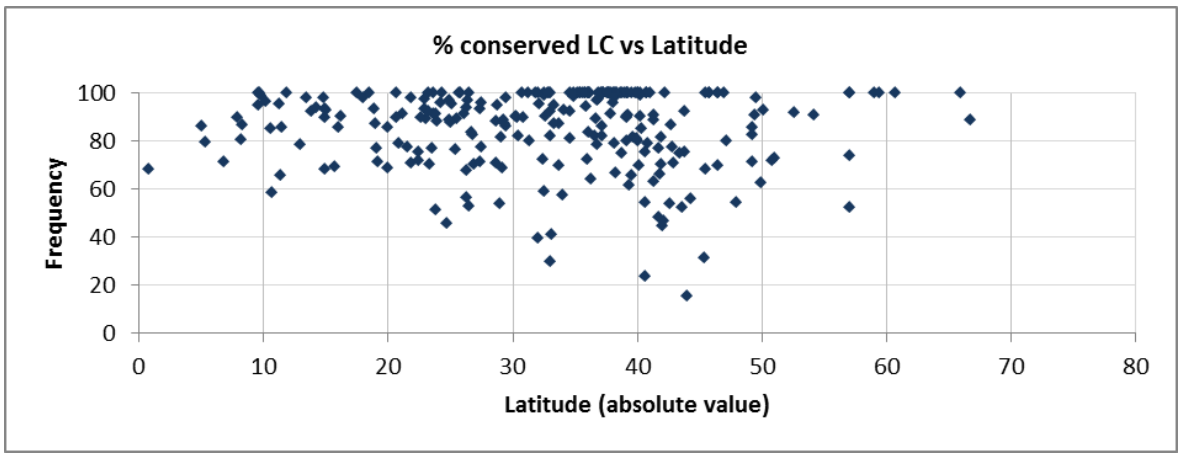

Figure 14: Percentage of conserved LC as a function of reservoir latitude. Latitudes are set to positive values

Reservoir Mean Depth

Figure 19 shows the histogram of depth distribution: 230 reservoirs among the 278 studied ones have their mean depth in the range 0-60 m. The percentage of conserved LC as a function of reservoir mean depth (Figure 20) does not show a clear trend, but deep reservoirs have no reservoirs with less than 60 % conserved LC. However, it does not seem to be any clear relationship between reservoir mean depth and buffer method validity.

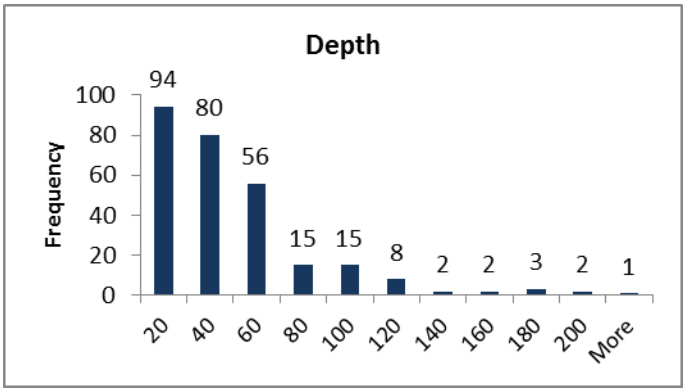

Figure 15: Histogram of depth distribution for the 278 reservoirs impounded after 1993

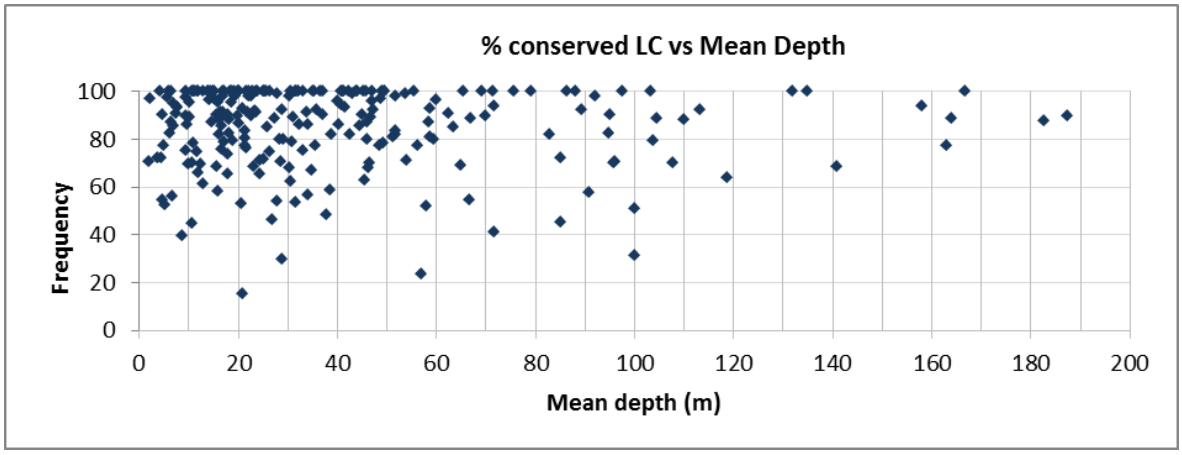

Figure 16: Percentage of conserved LC as a function of reservoir mean depth

Example of LC Distribution Provided by the Buffer Method: Three Gorges Reservoir

Figure 21 shows that there are four (LC labelled 6, 7, 10, 11) and three (LC labelled 7, 10, 11) dominant LC categories in the buffer and inundated area respectively when using the land cover categories. Figure 21 shows that there are three (LC Forest, Agriculture, Grassland/Shrubland) and two (LC Agriculture, Grassland/Shrubland) dominant LC classes in the buffer and inundated area respectively when using the GHG Screening Tool LC categories. The percentage of conserved LC between the inundated area and the buffer area is 71.9 if the AVHRR LC classification is used. When using the GHG Screening Tool LC classification, the percentage of conserved LC increases to 90 %.

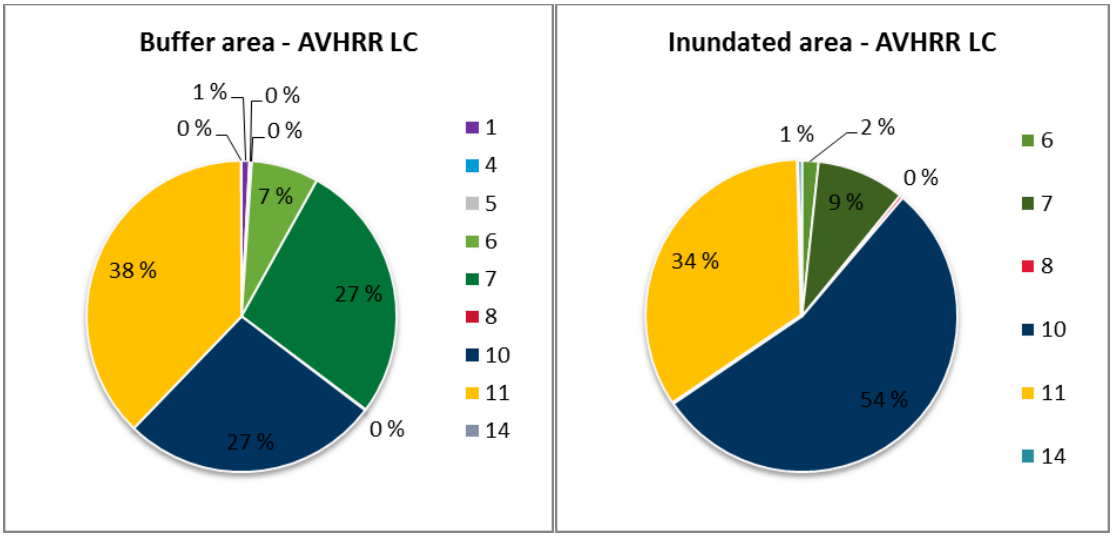

Figure 17:. LC distribution for the Three Gorges Reservoir in the buffer area (left) and in the inundated area (right). LC categories satellite data. The land cover type "water" use is not included

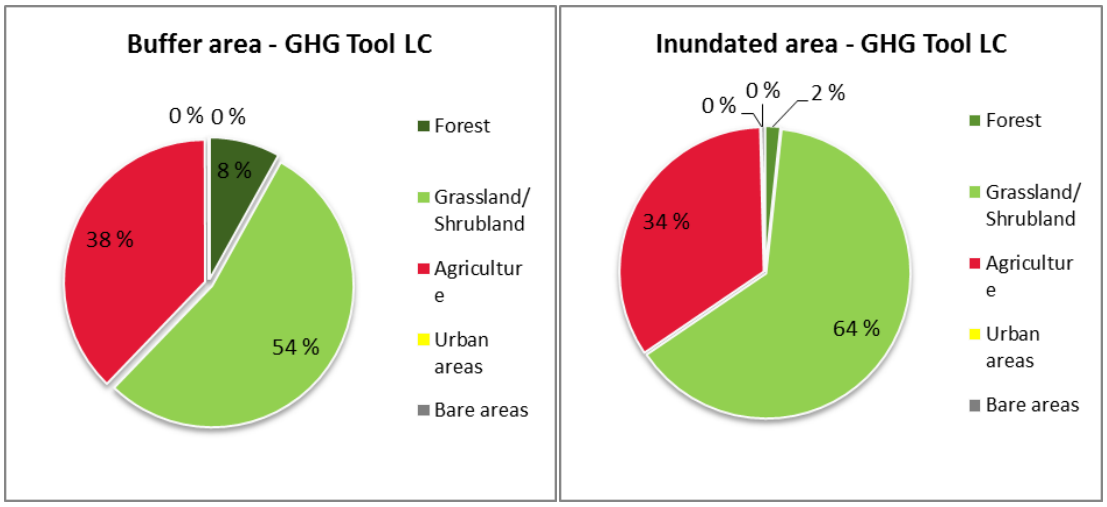

Figure 18: LC distribution for the Three Gorges Reservoir determined in the buffer area (left) and in the inundated area (right). LC categories from the GHG Screening Tool. The land cover with "water" use is not included

Annex X - **Construction Emission Factors**

Section 2.5 provides an overview of the calculations used to estimate construction emissions. These calculations rely on emissions factors to convert activity data to emissions data.

All the emissions factors used can be found in Table 13, Table 14, and Table 15. Some of the calculations require conversions to be undertaken, for example converting between volume and mass using a density. These conversions can be found in the kg/UoM (where UoM is 'Units of Measure') column in Table 13, and Table 14. Additionally, some of the calculations required assumptions to be made, for example the type of material used in an item. Details of these assumptions can be found in the note's column in all three tables.

Finally, some material types included an assumption regarding the distance they would be transported. These distances can be found in the Assumed Transport Distance (km) column of Table 14.

Table 13: Material (embodied, cradle to gate) emission factors for construction

Assessment Type	Category	Item	UoM	kg/UoM	EF1 kgCO2e/UoM	EF 1 Source	EF2 kgCO2e/UoM	EF 2 Source	EF Composite kgCO2e/UoM	Notes
Basic Assessment	**Earth and rockfill**		m3	2300	30.8	BC	11.648	ICE v2	21.224	ICE v2 and BC average Assumed 50/50 granular/rockfill
	Concrete		m3	2300	374.9	ICE v2	309.12	BC	342.01	ICE v2 and BC average - assumed Concrete, reinforced RC32_40/Cement concrete (road)
	Steel		t	1000	1950	ICE v2	3190	BC	2570	ICE v2 and BC average - assumed General - World Avg. Recy. Cont./Steel or tinplate (new)
Detailed Assessment	**Earthworks**	**Soft excavation**	m3	1460	N/A	N/A	N/A	N/A	0	No emissions
		Rock excavation	m3	2880	N/A	N/A	N/A	N/A	0	No emissions
		Clearance and removals	ha	N/A	N/A	N/A	N/A	N/A	0	No emissions
	Fill	**Granular fill**	m3	2240	11.648	ICE v2	30.8	BC	21.224	ICE v2 and BC average - assumed 50/50 granular/rockfill
		Rock armour	m3	2880	227.52	ICE v2	N/A	N/A	227.52	One Emissions factor - assumed stone general
		Zoned Rockfill	m3	2880	227.52	ICE v2	N/A	N/A	227.52	One Emissions factor - assumed stone general
		Rock bolts	nr	20	2890	ICE v2	3190	BC	60.8	ICE v2 and BC average - assumed virgin steel/Steel or tinplate (new) - based on 20kg bolts
	Concrete works	**Formwork**	m2	20.7	20.7	CESSM4	N/A	N/A	20.7	One Emissions factor - Formwork
		Facing Concrete	m3	2300	374.9	ICE v2	309.12	BC	342.01	ICE v2 and BC average - assumed Concrete, reinforced RC32_40/Cement concrete (road)
		Mass Concrete	m3	2300	220	ICE v2	N/A	N/A	220	One Emissions factor - assumed concrete, unknown mix
		Reinforced Concrete	m3	2300	374.9	ICE v2	459.77	BC	417.335	ICE v2 and BC average - assumed Concrete, reinforced RC32_40/Continuous reinforced concrete (road)
		Shotcrete	m2	220	22	ICE v2	N/A	N/A	22	One emissions factor - assumed concrete, unknown mix - based on thickness of 100mm
		Reinforcement	t	1000	1860	ICE v2	3190	BC	2525	ICE v2 and BC average - assumed Bar & rod - World Avg. Recy. Cont./Steel or tinplate (new)

Assessment Type	Category	Item	UoM	kg/UoM	EF1 kgCO2e/UoM	EF 1 Source	EF2 kgCO2e/UoM	EF 2 Source	EF Composite kgCO2e/UoM	Notes
	Steelworks	**Steel Penstocks**	t	1000	1860	ICE v2	3190	BC	2525	ICE v2 and BC average - assumed Bar & rod - World Avg. Recy. Cont./Steel or tinplate (new)
		Steel liner	t	1000	1950	ICE v2	3190	BC	2570	ICE v2 and BC average - assumed General - World Avg. Recy. Cont./Steel or tinplate (new)
		Miscellaneous Steelwork	t	1000	1950	ICE v2	3190	BC	2570	ICE v2 and BC average - assumed General - World Avg. Recy. Cont./Steel or tinplate (new)
	Roads and bridges	**New roads**	km	N/A	231750	ICE v2	550000	BC	390875	ICE v2 and BC average - assumed asphalt 7.5m wide/ TC2 or "normal" parking
		Refurbishment of existing roads	km	N/A	115875	ICE v2	275000	BC	195437.5	ICE v2 and BC average - assumed asphalt 7.5m wide/ TC2 or "normal" parking - based on refurbishment being half construction
		PCC vehicular bridge deck	m2	300	687.5	BC	N/A	N/A	687.5	One Emissions factor - assumed TC3 or "intense" parking - based on width of 7.5m
	Equipment	**Power generation equipment**	MW	18000	35100	ICE v2	N/A	N/A	35100	One Emissions factor - assumed Steel 33% recycled
		Power connection	kV	Calculated	N/A	N/A	N/A	N/A	Calculated	kg/UoM - (KV x 0.1111) + 112.17 / EFkgCO2e/UoM - (KV x 301.17) + 380101 - based on model

Table 14: Transport emission factors for construction

Assessment Type	Category	Item	UoM	kg/UoM	Assumed Transport Distance (km)	EF kgCO2e/t.Km	Source	Notes
Basic Assessment	**Earth and rockfill**		m3	2300	N/A	0.2035	GHG Protocol	Assumed average rigid HGV
	Concrete		m3	2300	N/A	0.2035	GHG Protocol	Assumed average rigid HGV
	Steel		t	1000	N/A	0.2035	GHG Protocol	Assumed average rigid HGV
Detailed Assessment	**Earthworks**	**Soft excavation**	m3	1460	N/A	0.2035	GHG Protocol	Assumed average rigid HGV
		Rock excavation	m3	2880	N/A	0.2035	GHG Protocol	Assumed average rigid HGV
		Clearance and removals	ha	N/A	N/A	0.2035	GHG Protocol	Assumed average rigid HGV
	Fill	**Granular fill**	m3	2240	N/A	0.2035	GHG Protocol	Assumed average rigid HGV
		Rock armour	m3	2880	N/A	0.2035	GHG Protocol	Assumed average rigid HGV
		Zoned Rockfill	m3	2880	N/A	0.2035	GHG Protocol	Assumed average rigid HGV
		Rock bolts	nr	20	N/A	0.2035	GHG Protocol	Assumed average rigid HGV
	Concrete works	**Formwork**	m2	20.7	150	0.2035	GHG Protocol	Assumed average rigid HGV
		Facing Concrete	m3	2300	N/A	0.2035	GHG Protocol	Assumed average rigid HGV
		Mass Concrete	m3	2300	N/A	0.2035	GHG Protocol	Assumed average rigid HGV
		Reinforced Concrete	m3	2300	N/A	0.2035	GHG Protocol	Assumed average rigid HGV
		Shotcrete	m2	220	N/A	0.2035	GHG Protocol	Assumed average rigid HGV
		Reinforcement	t	1000	N/A	0.2035	GHG Protocol	Assumed average rigid HGV
	Steelworks	**Steel Penstocks**	t	1000	N/A	0.2035	GHG Protocol	Assumed average rigid HGV
		Steel liner	t	1000	N/A	0.2035	GHG Protocol	Assumed average rigid HGV
		Miscellaneous Steelwork	t	1000	N/A	0.2035	GHG Protocol	Assumed average rigid HGV
	Roads and bridges	**New roads**	km	N/A	150	0.2035	GHG Protocol	Assumed average rigid HGV

Assessment Type	Category	Item	UoM	kg/UoM	Assumed Transport Distance (km)	EF kgCO2e/t.Km	Source	Notes
		Refurbishment of existing roads	km	N/A	150	0.2035	GHG Protocol	Assumed average rigid HGV
		PCC vehicular bridge deck	m2	300	250	0.2035	GHG Protocol	Assumed average rigid HGV
	Equipment	**Power generation equipment**	MW	18000	250	0.2035	GHG Protocol	Assumed average rigid HGV
		Power connection	kV	Calculated	250	0.2035	GHG Protocol	Assumed average rigid HGV

Table 15: Plant and equipment emission factors for construction

Assessment Type	Category	Item	UoM	EF kgCO2e/UoM	Source	Notes
Basic Assessment	**Earth and rockfill**		m3	1	CESMM4	Filling, E.06.01.04.01
	Concrete		m3	5.07	CESSM4	Placing of concrete, F.06.01.01.01
	Steel		t	N/A	N/A	No Emissions factor
Detailed Assessment	**Earthworks**	**Soft excavation**	m3	1.3529	CESMM4	E.04.02.07.01
		Rock excavation	m3	6.128	CESMM4	E.04.03.05.01
		Clearance and removals	ha	439.4	CESMM4	D.01.01.00.01
	Fill	**Granular fill**	m3	N/A	N/A	No Emissions factor
		Rock armour	m3	N/A	N/A	No Emissions factor
		Zoned Rockfill	m3	N/A	N/A	No Emissions factor
		Rock bolts	nr	N/A	N/A	No Emissions factor
	Concrete works	**Formwork**	m2	N/A	N/A	No Emissions factor
		Facing Concrete	m3	5.07	CESMM4	Placing of concrete, F.06.01.01.01
		Mass Concrete	m3	5.07	CESMM4	Placing of concrete, F.06.01.01.01
		Reinforced Concrete	m3	5.07	CESMM4	Placing of concrete, F.06.01.01.01
		Shotcrete	m2	5.07	CESMM4	Placing of concrete, F.06.01.01.01
		Reinforcement	t	N/A	N/A	No Emissions factor
	Steelworks	**Steel Penstocks**	t	N/A	N/A	No Emissions factor
		Steel liner	t	N/A	N/A	No Emissions factor
		Miscellaneous Steelwork	t	N/A	N/A	No Emissions factor
	Roads and bridges	**New roads**	km	N/A	N/A	No Emissions factor
		Refurbishment of existing roads	km	N/A	N/A	No Emissions factor
		PCC vehicular bridge deck	m2	N/A	N/A	No Emissions factor
	Equipment	**Power generation equipment**	MW	N/A	N/A	No Emissions factor
		Power connection	kV	N/A	N/A	No Emissions factor